Journal of South American Earth Sciences 32 (2011) 110–126

Contents lists available at ScienceDirect

Journal of South American Earth Sciences

journal homepage: www.elsevier.com/locate/jsames

Across-arc variation of the Famatinian magmatic arc (NW Argentina) exemplified by I-, S- and transitional I/S-type Early Ordovician granitoids of the Sierra de Velasco

Pablo Grosse [a,*], Laura I. Bellos [b], Camilo R. de los Hoyos [b], Mariano A. Larrovere [c], Juana N. Rossi [b], Alejandro J. Toselli [b]

[a] CONICET and Fundación Miguel Lillo, Miguel Lillo 251, (4000) San Miguel de Tucumán, Argentina
[b] Instituto Superior de Correlación Geológica – CONICET and Facultad de Ciencias Naturales, Universidad Nacional de Tucumán, Miguel Lillo 205, (4000) San Miguel de Tucumán, Argentina
[c] Departamento de Geociencias, CRILAR-CONICET and Universidad Nacional de La Rioja, Entre Ríos y Mendoza s/n, 5301 – Anillaco, La Rioja, Argentina

ARTICLE INFO

Article history:
Received 13 August 2010
Accepted 23 March 2011

Keywords:
I-type granitoids
S-type granitoids
Transitional I/S-type granitoids
Granitoid genesis
Famatinian magmatic arc

ABSTRACT

The Early Ordovician granitoids of the Sierra de Velasco reflect the across-arc compositional variation of the Famatinian magmatic arc (NW Argentina) developed along the proto-Andean margin of western Gondwana. This variation is characterized by means of field, petrographical, geochemical and isotopic studies. The Sierra de Velasco contains three main types of Early Ordovician granitoids that are mineralogically and geochemically distinct, but generally conform a continuous high-K, magnesian and calc-alkalic magmatic series. I-type granitoids (IG) make up the southern part of the range. They are biotite–hornblende–titanite metaluminous to weakly peraluminous granodiorites and tonalites typical of a coastal I-type belt and were possibly formed by melting of mafic lower crust/lithospheric mantle, with minor assimilation of crustal metasediments. S-type granitoids (SG) crop out in the central and northern portions of the range. They are biotite–muscovite and biotite–cordierite strongly peraluminous syeno- and monzogranites representative of an inland S-type belt and were possibly formed by large-scale anatexis of metasedimentary crust and hybridization with more mafic lower crustal melts. Between the IG and SG, in the central parts of the range, transitional I/S-type granitoids (TG) are recognized that consist of biotite, biotite–muscovite and subordinate biotite–titanite–allanite–epidote moderately peraluminous monzogranites, granodiorites and tonalites. The TG show intermediate characteristics and were possibly generated by less common mechanisms of mixing between I-type and S-type magmas and/or their parent mafic lower crustal and metasedimentary melts. The transition from IG to TG to SG towards the continental interior reflects a compositional continuum related to a progressive variation in the degrees of mixing between mafic and metasedimentary end-members.

1. Introduction

The Sierras Pampeanas of northwestern Argentina contain abundant Ordovician granitoid batholiths and meta-volcanic rocks that together define the Famatinian magmatic arc. This arc developed along the active proto-Andean margin of western Gondwana in response to the eastward subduction of a paleo-Pacific oceanic plate (e.g. Toselli et al., 1996; Pankhurst and Rapela, 1998; Miller and Söllner, 2005). The resulting granitoid magmatism is presently distributed along two main belts (Pankhurst et al., 2000): a metaluminous I-type belt towards the west, and a peraluminous S-type belt towards the east (Fig. 1). The I-type belt consists of Cordilleran-type granitoids (e.g. Pankhurst et al., 1998; Otamendi et al., 2009b), whereas the S-type belt has been regarded as an inner Cordilleran belt (e.g. Rapela et al., 1990; Toselli et al., 1996).

The across-arc dichotomy of coastal I-type granitoids and inland S-type granitoids is a common feature of many orogenic belts. The best-known example is that of western United States (e.g. Miller and Bradfish, 1980), where the I-type belt is represented by the Sierra Nevada and Peninsular Ranges batholiths and the S-type belt by inner Cordilleran muscovite-bearing granites, of which the main representative is the Idaho batholith. Other examples include the New England orogen of eastern Australia (Shaw and Flood, 1981), the Southeast Asian tin belt (Cobbing et al., 1986) and the middle and southern Urals (Fershater et al., 1998). The difference between

* Corresponding author. Tel.: +54 381 4239723.
E-mail address: pablogrosse@yahoo.com (P. Grosse).

0895-9811/$ – see front matter © 2011 Elsevier Ltd. All rights reserved.
doi:10.1016/j.jsames.2011.03.014

the two belts is generally attributed to an increased contribution of the continental crust towards the interior of the continent (e.g. Brown et al., 1984).

The Sierra de Velasco makes up one of the largest granitoid massifs of the Famatinian magmatic arc (Fig. 1) and has generally been considered part of the inner S-type belt in regional studies (e.g. Rapela et al., 1990; Toselli et al., 1996; Pankhurst et al., 2000). However, more recent local studies by Bellos et al. (2002) and Bellos (2005, 2008) have shown that the southern portion of the sierra consists of metaluminous granitoids belonging to the I-type belt (Figs. 1 and 2). The presence of both granitoid types along >150 km of continuous granitic outcrops makes the Sierra de Velasco an ideal area to study the transition between the I- and S-type granitoids across the Famatinian magmatic arc.

In this contribution, we present the results of field, petrographical, geochemical and isotopic studies of the Famatinian granitoids outcropping in the Sierra de Velasco. In addition to I- and S-type granitoids, we define and characterize intermediate or transitional I/S-type granitoids in this mountain range. We discuss the possible origins of each granitoid type and relate them to the geotectonic setting of this part of the western margin of Gondwana during the Early Paleozoic.

2. Geological setting

2.1. The Sierras Pampeanas and the Famatinian magmatic arc

The Sierras Pampeanas of NW Argentina consist in a series of basement blocks exhumed during the Neogene by high-angle, N–S trending reverse faults (González Bonorino, 1950) related to the subduction of the Nazca plate under the western margin of South America (Jordan and Allmendinger, 1986; Isacks, 1988). These blocks are made up almost entirely of metamorphic and intrusive rocks of Neoproterozoic to Early Carboniferous age. The evolution of the Sierras Pampeanas during the Neoproterozoic and Paleozoic is characterized by two main periods of convergence along the proto-Pacific margin of Gondwana that generated two main orogenic cycles: the Pampean and Famatinian cycles (Aceñolaza and Toselli, 1973, 1981). Each cycle spans distinctive depositional, metamorphic, deformational and magmatic events.

The Pampean Cycle (~580–520 Ma) began with the deposition of an extensive pelite-greywacke turbiditic sequence in a passive margin setting (e.g. Ramos, 1988; Ježek, 1990; Sims et al., 1998; Rapela et al., 1998; Do Campo and Guevara, 2005). These sediments, and their metamorphic equivalents, make up the Puncoviscana Formation, originally defined by Turner (1960) in the extreme NW of Argentina, but later extended to encompass most of the metamorphic rocks of the Sierras Pampeanas (e.g. Aceñolaza and Toselli, 1981; Toselli, 1990; Prozzi, 1990; Willner et al., 1990; Sims et al., 1998; Von Gosen and Prozzi, 1998). Metamorphism, deformation and calc-alkaline magmatism affected the Puncoviscana Formation at ca. 530–520 Ma (e.g. Lork et al., 1990; Adams et al., 1990; Rapela et al., 1998), probably in a collisional setting that included subduction, accretion of the Pampean terrane, and late- to post-orogenic extensional collapse (e.g. Rapela et al., 1998).

The Famatinian Cycle (ca. 490–350 Ma) began with the deposition of siliciclastic sediments in extensional marine basins between the Middle/Late Cambrian and Early Ordovician

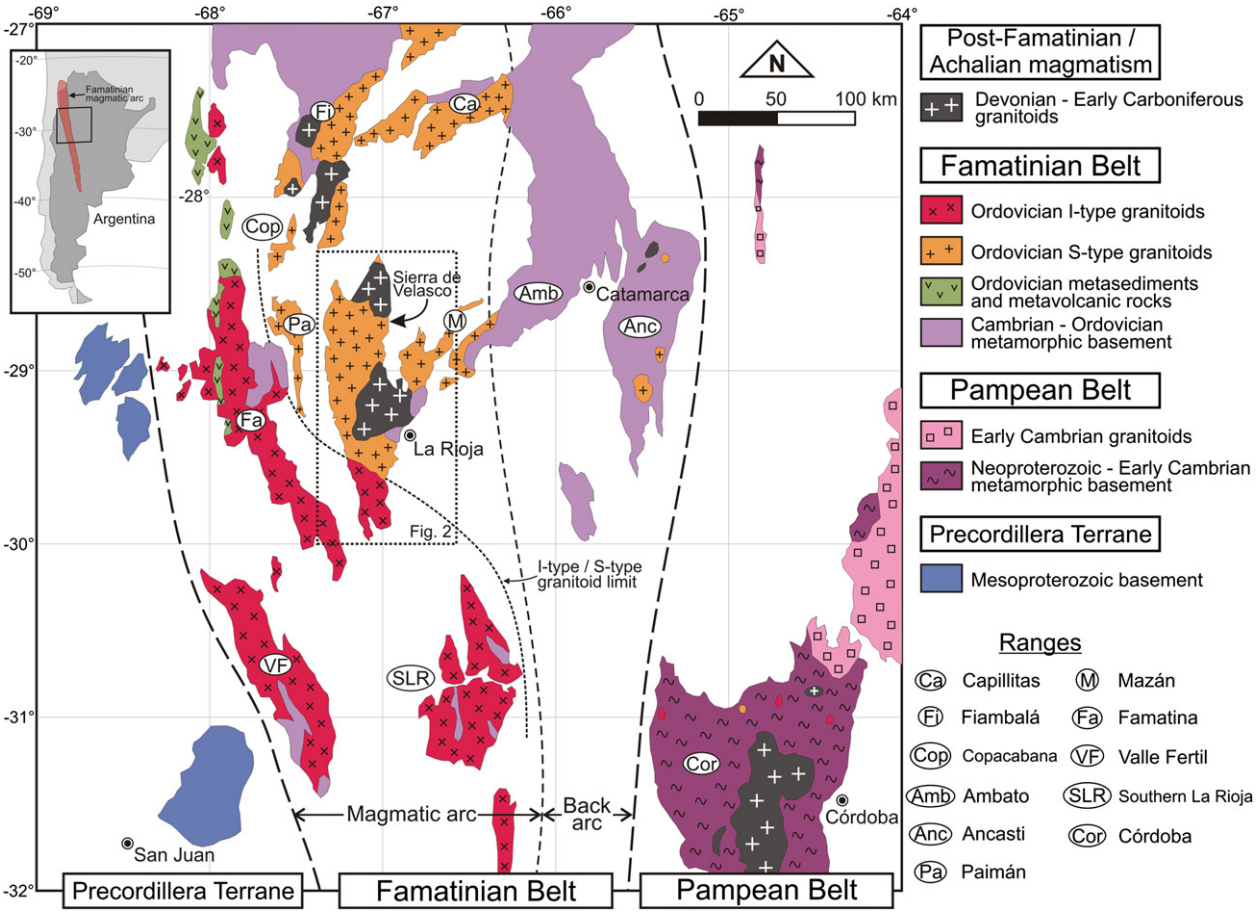

Fig. 1. General geological map of the central part of the Sierra Pampeanas of NW Argentina between 27°S and 32°S. Inset shows map location and extent of the Famatinian magmatic arc (modified from Chernicoff et al., 2010). Dotted rectangle indicates location of Fig. 2.

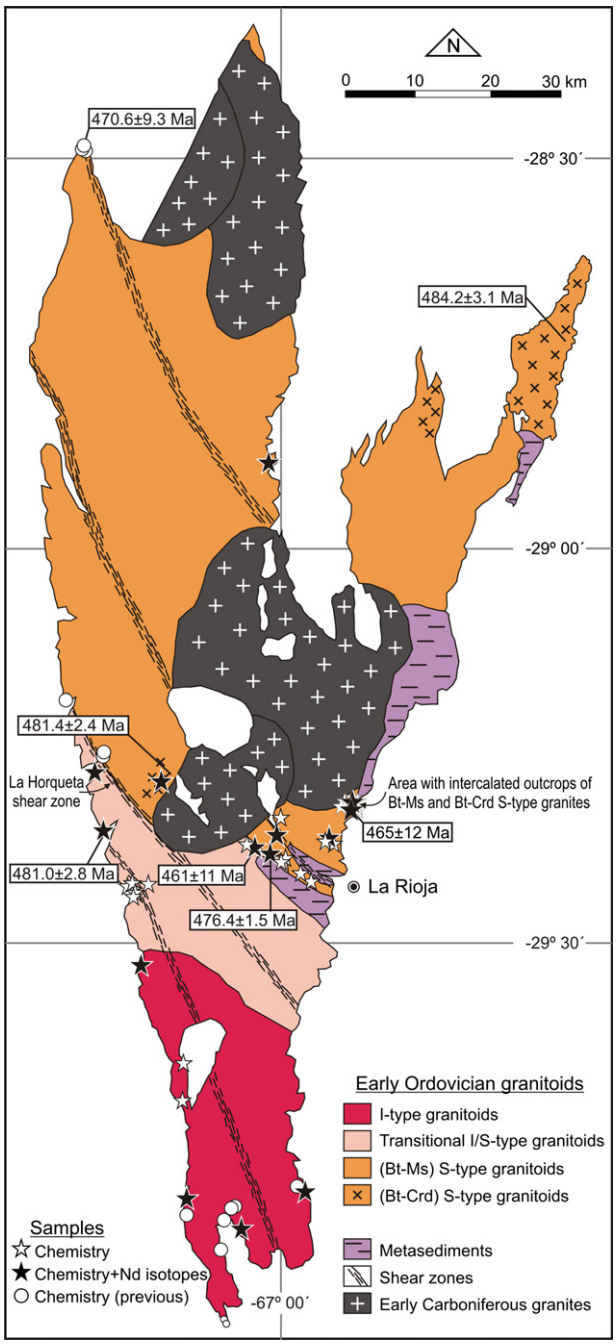

Fig. 2. Geological map of the Sierra de Velasco. Location of samples used in this study and of existing U–Pb ages are shown. Previous geochemistry samples are from Bellos (2005), Rossi et al. (2005) and López et al. (2007). U–Pb ages are from Pankhurst et al. (2000), Rapela et al. (2001), Báez et al. (2008) and de los Hoyos et al. (in press); see text for details. Mineral abbreviations throughout the text are from Whitney and Evans (2010).

(e.g. Bahlburg and Hervé, 1997; Bahlburg, 1998; Bock et al., 2000). The resulting sequences form thick sedimentary packages that lie discordantly over the Puncoviscana Formation. Renewed plate convergence and subduction caused superimposed high T/P metamorphism spanning the interval ca. 480–430 Ma (e.g. Bachmann et al., 1986; Sims et al., 1998; Lucassen and Becchio, 2003; Büttner et al., 2005; Larrovere et al., 2011; de los Hoyos et al., in press) and the development of the Famatinian magmatic arc along the continental margin of western Gondwana. It is widely accepted that Famatinian magmatism preceded the collisional accretion of the Precordillera terrane (i.e. Cuyania, Fig. 1) in Mid-Ordovician times (e.g. Ramos, 1988, 2004; Astini et al., 1995; Pankhurst et al., 1998; Thomas and Astini, 2003; Vaughan and Pankhurst, 2008), although debate still continues as to its origin (e.g. Aceñolaza et al., 2002).

The Famatinian magmatic arc is presently found as a NNW-SSE trending belt occupying over 1500 km along strike from ~22°S to ~33°S (Fig. 1) within the Sierras Pampeanas and extending northwards into the Puna–Altiplano region, where Famatinian rocks switch from plutonic to volcanic (e.g. Coira et al., 1999; Viramonte et al., 2007). Further south, the Famatinian arc is mostly buried beneath Quaternary sediments but can be followed down to ~39°S on aeromagnetic data (Chernicoff et al., 2010, Fig. 1). The Famatinian arc is characterized by widespread magmatism that formed an outer I-type dominated belt and an inner S-type dominated belt (Pankhurst et al., 2000, Fig. 1). In the Sierras Pampeanas, the I-type belt is represented mainly by the sierras of Famatina (e.g. Aceñolaza et al., 1996; Saavedra et al., 1998), southern La Rioja (Chepes, Los Llanos and Ulapes, e.g. Pankhurst et al., 1998) and Valle Fértil (e.g. Otamendi et al., 2009b). The S-type belt is represented mainly by the sierras of Fiambalá (e.g. Grissom et al., 1998), Capillitas (e.g. Rossi et al., 2002), Mazán (e.g. Schalamuk et al., 1989; Toselli et al., 1991) and Velasco (see Section 2.2). This across-arc feature can also be found in the Puna–Altiplano region, where the Ordovician plutonic and volcanic rocks have been separated into the metaluminous I-type "Faja Eruptiva Occidental" to the west and the peraluminous S-type "Faja Eruptiva Oriental" to the east (e.g. Coira et al., 1999; Poma et al., 2004; Viramonte et al., 2007).

U–Pb zircon geochronology (by both conventional and SHRIMP methods) constrains Famatinian magmatism to the Early Ordovician (between 490 and 460 Ma) for both the I-type (Pieters et al., 1997; Pankhurst et al., 1998, 2000; Dahlquist et al., 2008; Chernicoff et al., 2010) and S-type belts (Pankhurst et al., 2000; Rapela et al., 2001; Höckenreiner et al., 2003; Viramonte et al., 2007; Varela et al., 2008). The existing ages do not reveal any progressive migration of activity, but rather indicate that both belts are essentially contemporaneous.

A subsequent magmatic phase occurred during the Middle Devonian to Early Carboniferous (e.g. Rapela et al., 1991; Grissom et al., 1998; Llambías et al., 1998; Siegesmund et al., 2004; Dahlquist et al., 2006, 2010; Steenken et al., 2008; Grosse et al., 2009). This magmatism has been related either to a post-orogenic period at the end of the Famatinian Cycle (e.g. Llambías et al., 1998; Pankhurst and Rapela, 1998; Miller and Söllner, 2005), or to a new cycle called the Achalian Cycle (e.g. Sims et al., 1998; Dahlquist et al., 2006).

2.2. The Sierra de Velasco

The Sierra de Velasco is made up almost exclusively of granitic rocks. A metamorphic basement is only present as small outcrops of metasedimentary rocks along the eastern flank of the sierra (Fig. 2). These rocks can be correlated with the La Cébila Formation, defined by González Bonorino (1951) in the Sierra de Ambato, to the northeast (Fig. 1). The La Cébila Formation is essentially metapelitic and comprises schists, phyllites and subordinated interbedded meta-quartzites. The depositional age of this unit is constrained between ca. 530 Ma, which corresponds to the youngest detrital zircons dated by Finney et al. (2003, 2004) and Rapela et al. (2007), and ca. 480 Ma, which corresponds to the oldest granitoids of the sierras of Velasco and Mazán. The recent discovery of marine fossils in this formation further constrains its depositional age to the Early Ordovician (Verdecchia et al., 2007), very close to the ages of the

granites that intrude the formation. In addition, migmatites and hornfelses can be found in the vicinity of the granitic intrusives.

The Sierra de Velasco contains granitoids of two main ages, Early Ordovician and Early Carboniferous (e.g. Báez et al., 2005; Toselli et al., 2005, 2007). The Early Ordovician granitoids are spatially dominant (Fig. 2) and are the subject of this paper. Pankhurst et al. (2000) analyzed these granitoids in a regional context and considered them part of the S-type Famatinian belt, but recognized that the "biotite granites" of the southwestern part of the range have geochemical trends and compositions that suggest hybridization with I-type melts. In more local studies carried out at the northwestern (Rossi et al., 2000, 2005) and southern (Bellos, 2005, 2008) ends of the range, the northwestern granitoids were defined as S-type and the southern granitoids as I-type. The transition between the two granitoid types in the central part of the sierra has not been previously addressed.

Several U–Pb age determinations exist for Early Ordovician granitoids of the Sierra de Velasco (Fig. 2). Pankhurst et al. (2000) obtained an age of 481.0 ± 2.8 Ma (U–Pb SHRIMP on zircon) for a two-mica granite on the western flank of the sierra (here considered part of the transitional I/S-type granitoid group, see Section 3). They also obtained an age of 484.2 ± 3.1 Ma for a cordierite S-type granite from neighboring Sierra de Mazán. Rapela et al. (2001) obtained an age of 481.4 ± 2.4 Ma (using the same method) for a biotite-cordierite S-type granitoid located in the central region of the Sierra de Velasco. More recently, Báez et al. (2008) obtained an age of 470.6 ± 9.3 Ma (conventional U–Pb on zircon) for the biotite–muscovite S-type granitoid cropping out at the northwestern tip of the sierra. Finally, de los Hoyos et al. (in press) report three ages for granitoids from the central-eastern flank: 461 ± 11 Ma (conventional U–Pb on zircon) for a transitional I/S-type granitoid, 476.4 ± 1.5 Ma (conventional U–Pb on monazite) for a biotite–muscovite S-type granitoid, and 465 ± 12 (conventional U–Pb on monazite) for a biotite–cordierite S-type granitoid (Fig. 2). No geochronological data exist for the I-type granitoids in the southern part of the sierra. However, their similarity with the granitoids of the sierras of Famatina and southern La Rioja suggests that they have comparable ages.

The Early Ordovician granitoids are cut by numerous NNW–SSE trending shear zones (Fig. 2) that also affect other ranges further north (e.g. López and Toselli, 1993; López et al., 2006, 2007; Höckenreiner et al., 2003). These shear zones dip sub-vertically towards the northeast and consist of mylonites and proto-mylonites. Kinematic indicators suggest compressional movements towards the southwest with a secondary sinistral transcurrent component (López et al., 2006). The shear zones of the Sierra de Velasco have not been dated. However, age determinations have been performed on similar mylonites located in the Sierra de Copacabana (Fig. 1) that are a continuation of the Velasco shear zones. López et al. (2000) obtained a K–Ar age of 436.3 ± 10.3 Ma on muscovites from a pegmatite within a shear zone, whereas Höckenreiner et al. (2003) obtained an Sm–Nd age of 402.0 ± 2.0 Ma on syntectonic garnets from mylonites.

In the northern and central-eastern sectors of the Sierra de Velasco, post-tectonic Early Carboniferous granites intrude the Ordovician granitoids and cross-cut the shear zones (e.g. Báez et al., 2002; Grosse and Sardi, 2005; Dahlquist et al., 2006, 2010; Grosse et al., 2009) (Fig. 2). These are high-K peraluminous, porphyritic syeno- and monzogranites emplaced in a post-orogenic to anorogenic setting.

3. Granitoid types, field relationships and petrography

Three main types of Famatinian granitoids can be recognized in the Sierra de Velasco based on their mineralogy and geochemistry (Fig. 2): metaluminous to weakly peraluminous biotite -hornblende -titanite I-type granitoids (IG), moderately peraluminous biotite–(muscovite)–(titanite) transitional I/S-type granitoids (TG), and strongly peraluminous biotite–(muscovite)–(cordierite) S-type granitoids (SG). Contact relationships between the granitoid types are usually not clear. The contact between the IG and the TG seems to be gradational. On the western flank of the sierra, the contact between the SG and the TG coincides with the La Horqueta shear zone (López et al., 2007, Fig. 2), whereas on the eastern flank it does not, but is obscured by the presence of metasediment outcrops.

3.1. I-type granitoids (IG)

The IG (i.e. Palanche pluton in the sense of Bellos, 2008) consist of medium- to coarse-grained biotite–hornblende granodiorites and tonalites, and subordinate biotite monzogranites. They are equigranular to slightly porphyritic, with occasional K-feldspar megacrysts (5–20%). Their mineral assemblage consists of plagioclase (23–59%), quartz (20–46%), K-feldspar (3–25%), biotite (3–19%), hornblende (3–10%), titanite (<4%), allanite (<3%), opaque minerals (<1%, mostly magnetite), epidote, apatite and zircon. Plagioclase is subhedral to anhedral, has albite twinning and frequently shows optical oscillatory zoning. K-feldspar is scarce, perthitic and interstitial in the tonalities, whereas in the granodiorites it is sometimes present as light pink megacrysts up to 2–3 cm across. Biotite is subhedral to anhedral, has light brown to green pleochroism and is partially altered to epidote, muscovite and chlorite. Hornblende is subhedral to anhedral, has light to dark green pleochroism, and is sometimes altered to epidote. Titanite is associated either with biotite or hornblende and occurs as small rhombic-shaped euhedral to subhedral crystals. Allanite is anhedral to subhedral, generally prismatic, and is normally enclosed by epidote. Opaque minerals are associated with biotite, hornblende and titanite. Apatite occurs as prismatic inclusions in quartz, plagioclase and biotite, whereas zircon is included mostly in biotite forming small prismatic crystals with pleochroic haloes.

The IG can exhibit weak to moderate deformation. Quartz crystals have ondulose extinction and commonly show fine-grained recrystallized borders, feldspar twins are sometimes slightly deformed, and biotites show kinked cleavages.

The IG contain mafic enclaves, syn-plutonic dykes and small mafic intrusives. All of these mafic rocks show signs of hybridization with the granitoids. Enclaves have sizes usually between 10 and 50 cm, rounded borders and oval shapes. Contacts with the host granitoids can be sharp, lobate, cuspate or sometimes diffuse. Schlieren commonly occur around their borders and they contain xenocrysts from the host granitoid. The dykes have variable strike and thickness, generally between 0.3 and 10 m. They are commonly disrupted and fragmented, sometimes forming enclave swarms. The contacts with the enclosing granitoids are sharp and they are normally bordered by hybrid rocks of intermediate composition. The intrusives have irregular shapes and sizes between 2 and 10 m; they are composed of dioritic cores and hybrid granodiorite shells. Both enclaves and dykes have quartz-dioritic composition, sometimes grading to tonalitic or dioritic. They are dark colored and have a fine-grained, equigranular texture. They are mainly composed of evenly distributed subhedral plagioclase (45–65%), pale brown to green hornblende (5–45%) and brown biotite (up to 25%). Hornblende also occurs as clots. Quartz and K-feldspar are scarce and interstitial or occur as xenocrysts from the enclosing granitoid, normally surrounded by hornblende forming ocellar textures. Subhedral titanite and opaque minerals, mostly magnetite, are common. Apatite is abundant as small elongate prisms and needles. No large mafic bodies are found in the IG, in contrast with other areas of the I-type granitic belt such as the western part of the

Sierra de Famatina (Aceñolaza et al., 1996) and the Sierra de Valle Fértil (Otamendi et al., 2009a, b). The IG also contain scarce, greenschist facies metamorphic xenoliths formed by quartz, K-feldspar and biotite.

3.2. Transitional I/S-type granitoids (TG)

The TG are normally dark gray, medium- to coarse-grained equigranular granodiorites and tonalites, but can grade to pinkish-gray porphyritic monzogranites. The only abundant accessory mineral is biotite. Muscovite is usually present, whereas hornblende is never observed, except within mafic magmatic enclaves. Typical modal compositions are quartz (30–35%), plagioclase (25–45%), K-feldspar (5–20%), biotite (10–25%), muscovite (0–7%), apatite (1%), zircon, monazite and opaque minerals (magnetite and ilmenite). Plagioclase forms subhedral laths with albite twinning and oscillatory zoning. K-feldspar normally forms small interstitial crystals. In the porphyritic variety, K-feldspar also occurs as pink megacrysts of up to 10 cm across and can reach abundances of 10%. Biotite occurs as subhedral, brown to green laminar crystals, usually grouped in elongated bands, together with scarce muscovite. Apatite is relatively abundant and occurs as equidimensional, subhedral crystals always in contact with, or included in, biotite. Small prismatic zircon crystals are generally included in biotite or more rarely in plagioclase. Subhedral to anhedral monazite grains were only recognized in mineral concentrates. A subordinate variety of the TG is characterized by the absence of muscovite and the occurrence of epidote, allanite and titanite (0.5–1%) in association with biotite. In this variety, epidote is subhedral to euhedral and equidimensional, whereas allanite forms subhedral and elongated prismatic crystals, and titanite occurs as light brown, euhedral, rhombic-shaped grains.

The TG generally show stronger deformation than the IG. A foliated structure is commonly observed, consisting of larger quartz and plagioclase crystals surrounded by smaller recrystallized quartz and biotite crystals forming sub-parallel bands. Feldspars usually show discontinuous and bent twinning, whereas micas are commonly kinked. Rossi and Toselli (2004) suggest that greenschist facies metamorphic conditions were reached, close to the brittle-ductile boundary at ~12 km (Sibson, 1977).

Both metasedimentary and mafic magmatic enclaves are found in the TG. Metasedimentary enclaves composed of schists, phyllites and hornfelses occur either as small enclaves or as large roof pendants. Contacts between the TG and metasedimentary host-rocks and enclaves are frequently irregular and partly diffuse, indicating relatively deep emplacement levels compared to thebiotite-cordierite SG (see Section 3.3). The hornfels paragenesis is quartz+K-feldspar+biotite+plagioclase+cordierite+sillimanite+garnet. Rossi and Toselli (2004) concluded that hornfel septas within the TG on the western flank of the Sierra de Velasco equilibrated at 640°C and 4.8kbar. Mafic magmatic enclaves are similar to those found in the IG but are less abundant. They decrease in both abundance and size from south (close to the IG) to north. They are quartz-dioritic to tonalitic and consist of hornblende+biotite+plagioclase+quartz+titanite±epidote±allanite.

3.3. S-type granitoids (SG)

The SG are medium- to coarse-grained porphyritic monzo- and syenogranites. Two varieties can be distinguished: a main biotite–muscovite variety and a subordinate biotite–cordierite variety (Fig. 2).

The biotite–muscovite variety (i.e. the Antinaco Orthogneiss in the sense of Rossi et al., 2000, 2005) is characterized by large (up to 10 cm) and abundant (10–20%) pink, perthitic K-feldspar megacrysts. These are commonly poikilitic (with inclusions of plagioclase and biotite) and show Carlsbad twinning. The matrix is composed of quartz (20–40%), zoned and unzoned plagioclase (15–30%), perthitic K-feldspar (30–40%), red-brown biotite (7–15%) and muscovite (2–10%), together with occasional garnet and scarce apatite, tourmaline, zircon, monazite and opaque minerals. Garnet is considered to be of magmatic origin because of its relatively high spessartite content that increases towards the rims (Rossi et al., 2005). Biotite + muscovite + garnet + plagioclase + aluminosilicate (kyanite/sillimanite) + quartz assemblages in the biotite-muscovite SG from the northwestern flank of the Sierra de Velasco yielded maximum temperatures and pressures of 591 °C and 4.3 kbar (Rossi et al., 2005).

The biotite–cordierite variety is found as relatively small bodies in the Sierra de Velasco (Fig. 2), whereas it forms large plutons in the sierras of Mazán and Capillitas (Figs. 1 and 2). Syenogranites are the most common facies, with subordinate monzogranites and granodiorites. This variety is also porphyritic, but the K-feldspar megacrysts are gray to pale-yellow. The matrix is formed by quartz (20–40%), unzoned plagioclase (15–30%), perthitic K-feldspar (20–40%), red-brown biotite (8–15%), cordierite (3–15%), sillimanite (<1–5%) and scarce garnet, apatite, zircon, monazite and opaque minerals (ilmenite and pyrite). Cordierite occurs as subhedral to euhedral prisms (up to 20 mm long) with very variable degrees of alteration. Three types of cordierite can be distinguished: (1) with aligned, fine-grained quartz and biotite inclusions in the cores and inclusion-free rims; (2) with unaligned coarse-grained inclusions of quartz, biotite and muscovite; and (3) inclusion-free. Simple twinning, considered indicative of a magmatic origin, is observed in types (2) and (3). Sillimanite is found associated with micas, either as euhedral prisms or showing fibrous habit. Monazite is relatively abundant and easily recognizable in backscattered images.

The SG normally show strong deformation and can be considered orthogneisses. The K-feldspar megacrysts are commonly deformed, producing asymmetrical structures. Feldspars in the matrix show discontinuous and bent twinning whereas quartz occurs both as larger crystals with ondulose extinction and as smaller recrystallized grains in a mosaic arrangement. Micas are fractured and oriented in sub-parallel bands. In the biotite–muscovite SG variety, both sillimanite and kyanite are found generated at the expense of quartz and muscovite (Rossi et al., 2000).

Enclaves are less abundant than in the IG and TG. Both metasedimentary and mafic magmatic types are found. In some areas, the biotite–cordierite SG variety contains abundant metasedimentary xenoliths and large roof pendants composed of phyllites and schists. The angular shape, sharp contacts and nearly unaltered metasedimentary textures and structures observed in most xenoliths and roof pendants indicate very shallow emplacement levels for the biotite–cordierite SG variety. Hornfels with the assemblage cordierite + biotite + K-feldspar + sillimanite + quartz occur only in the vicinity of the cordierite-bearing granitoids. Magmatic enclaves are less mafic than in the southern granitoids, their composition being biotitic tonalites.

4. Geochemistry

32 New whole-rock chemical analyses of samples from the studied granitoid types (3 of IG; 10 of TG; 19 of SG) are shown in Table 1; locations are shown in Fig. 2. Six samples were analyzed at Activation Laboratories Ltd. (Canada) by ICP (for major elements) and ICP-MS (for trace elements). The other 26 samples were analyzed at the universities of Oviedo (major elements) and Huelva

Table 1
Whole-rock major and trace element geochemistry of the studied Sierra de Velasco granitoids.

Sample:	I-type granitoids					Transitional I/S-type granitoids											
	6496[a]	6480[a]	7479	Avg. (14)	St. dev.	6554[a]	6575[a]	6553[a]	6564[a]	7466	7468	7603	7655	7920	7922	Avg. (12)	St. dev.
Mayor oxides (wt.%)																	
SiO_2	72.52	69.07	70.03	66.92	3.55	65.39	69.02	68.00	64.58	62.66	66.51	65.18	68.69	68.16	69.33	67.18	2.26
TiO_2	0.31	0.53	0.44	0.63	0.22	0.79	0.52	0.52	0.65	0.99	0.60	0.71	0.41	0.57	0.39	0.59	0.17
Al_2O_3	13.20	14.15	13.93	14.98	1.01	15.41	14.66	15.31	15.41	16.17	14.88	14.97	14.10	14.76	14.29	14.91	0.60
$Fe_2O_3^{tot}$	2.26	4.30	3.16	4.46	1.40	5.73	4.25	4.08	5.22	7.00	4.99	5.06	3.23	3.77	3.17	4.53	1.12
MgO	0.70	1.35	1.03	1.44	0.51	2.00	1.62	1.55	2.09	2.14	1.70	1.75	1.02	1.06	0.85	1.52	0.44
MnO	0.03	0.09	0.08	0.09	0.03	0.09	0.09	0.08	0.09	0.13	0.08	0.13	0.09	0.08	0.09	0.09	0.02
CaO	1.81	3.65	2.93	3.55	1.04	3.19	2.73	2.81	3.01	3.34	2.53	2.14	0.89	1.57	2.78	2.52	0.70
Na_2O	2.31	2.77	2.84	3.01	0.29	2.72	2.53	2.79	3.14	3.17	2.36	2.72	1.99	2.26	3.06	2.66	0.36
K_2O	5.04	2.72	3.93	3.32	1.01	3.45	3.50	3.63	3.16	2.93	4.50	3.47	6.38	5.66	3.46	4.03	1.05
P_2O_5	0.07	0.16	0.13	0.17	0.07	0.37	0.17	0.19	0.24	0.46	0.28	0.21	0.11	0.29	0.10	0.23	0.11
P.F.	1.16	1.09	0.56	0.90	0.29	1.19	1.29	1.22	1.10	0.78	0.71	n.d.	n.d.	n.d.	n.d.	0.91	0.33
Total	99.40	99.88	99.06	99.41	0.48	100.32	100.38	100.17	98.68	99.76	99.15	96.34	96.91	98.18	97.52	98.87	1.36
A/(CNK)	1.05	1.00	0.98	1.00	0.04	1.10	1.14	1.12	1.10	1.12	1.11	1.24	1.20	1.16	1.03	1.12	0.05
Trace elements (ppm)																	
V	46	84	54	86	36	108	75	64	91	110	n.d.	102	67	50	49	78	22
Cr	n.d.	60	188	51	45	63	37	42	62	79	n.d.	56	48	34	46	52	13
Rb	228	148	101	134	39	206	160	176	213	181	n.d.	189	181	167	143	177	23
Sr	119	133	118	184	50	93	85	92	90	84	n.d.	128	117	70	114	97	18
Y	34	41	26	32	8	42	33	26	28	28	n.d.	27	17	25	12	27	8
Zr	101	200	n.d.	210	54	228	175	123	165	n.d.	n.d.	185	158	161	120	164	34
Nb	18	14	10	13	3	24	15	14	26	28	n.d.	26	17	10	11	18	6
Ba	836	459	468	786	355	343	242	241	182	108	n.d.	404	731	334	385	344	168
La	18	51	29	53	49	37	31	23	28	27	n.d.	39	24	43	25	32	7
Ce	39	98	62	108	91	77	62	49	59	56	n.d.	91	60	108	60	70	18
Pr	5.2	10	8.3	11	7.6	9.9	7.7	5.9	6.7	7.5	n.d.	10	6.6	13	6.4	8.5	2.2
Nd	25	35	34	41	25	36	28	22	28	31	n.d.	37	24	48	23	32	8
Sm	8.1	6.5	6.7	8.4	3.0	8.0	6.1	4.8	6.0	7.2	n.d.	7.3	4.7	10.6	4.3	6.7	1.8
Eu	1.3	1.3	1.1	1.5	0.3	1.1	0.9	0.9	1.0	1.0	n.d.	1.3	1.1	0.9	0.9	1.1	0.2
Gd	8.4	6.0	5.8	7.1	1.7	7.0	5.2	4.2	5.7	7.3	n.d.	6.4	4.0	9.6	3.7	6.1	1.8
Tb	1.5	1.1	0.9	1.2	0.3	1.4	1.0	0.8	1.1	1.4	n.d.	1.1	0.7	1.4	0.5	1.0	0.3
Dy	8.3	6.8	5.3	6.2	1.6	8.3	6.1	4.7	5.7	7.2	n.d.	6.1	3.7	6.8	2.9	5.9	1.7
Ho	1.5	1.5	1.1	1.2	0.4	1.5	1.2	0.9	1.1	1.2	n.d.	1.1	0.7	1.2	0.5	1.1	0.3
Er	3.9	4.2	3.0	3.6	1.1	4.0	3.3	2.4	2.7	2.6	n.d.	2.7	1.9	2.6	1.3	2.7	0.7
Tm	0.58	0.71	0.43	0.55	0.17	0.61	0.55	0.38	0.41	0.32	n.d.	0.32	0.26	0.31	0.15	0.38	0.13
Yb	3.2	4.4	2.7	3.4	1.0	3.6	3.2	2.4	2.5	1.6	n.d.	1.8	1.6	1.7	0.8	2.2	0.8
Lu	0.41	0.83	0.39	0.47	0.17	0.49	0.48	0.33	0.35	0.22	n.d.	0.22	0.24	0.24	0.12	0.31	0.12
Ta	8.0	5.1	1.7	3.0	2.5	4.5	3.9	5.4	5.1	4.6	n.d.	2.7	2.9	2.3	2.5	3.7	1.1
Pb	28	18	17	18	5	16	14	24	22	16	n.d.	33	47	41	32	27	10
Th	8.1	17	16	14	8	20	18	12	12	12	n.d.	17	13	22	9.2	16	5
U	1.4	2.2	1.2	1.8	0.9	2.1	1.6	2.3	2.6	1.0	n.d.	1.8	1.9	0.7	1.0	1.7	0.6

Sample:	S-type Bt–Ms granitoids															S-type Bt–Crd granitoids							
	7688	7359	7721	7907	7908	7956	7581	7595	7833	7915	7610	7668	7913	Avg. (17)	St. Dev.	7493	7661	7663	7903	7905	7196	Avg. (7)	St. Dev.
Mayor oxides (wt.%)																							
SiO_2	71.02	71.99	69.46	72.85	75.13	72.55	72.41	72.09	69.54	70.80	72.91	73.98	73.61	71.46	2.23	68.85	66.64	73.23	73.34	74.70	72.00	71.29	2.85
TiO_2	0.43	0.36	0.51	0.24	0.13	0.26	0.24	0.12	0.40	0.33	0.25	0.20	0.24	0.35	0.17	0.63	0.71	0.22	0.31	0.28	0.49	0.44	0.18
Al_2O_3	14.54	14.27	15.00	14.09	14.19	14.48	13.78	13.85	14.23	14.04	14.17	14.13	14.27	14.30	0.43	14.68	16.09	14.68	14.33	13.55	14.28	14.56	0.77
$Fe_2O_3^{tot}$	3.66	2.88	4.10	2.21	1.13	2.22	1.52	1.46	3.20	2.60	1.60	1.88	2.23	2.84	1.23	4.51	4.55	1.26	1.86	1.29	3.75	3.01	1.48
MgO	1.17	0.87	1.36	0.51	0.24	0.58	0.05	0.16	0.88	0.54	0.50	0.40	0.49	0.81	0.53	1.56	1.70	0.44	0.54	0.43	1.22	1.01	0.54
MnO	0.10	0.09	0.10	0.03	0.01	0.04	0.02	0.03	0.09	0.07	0.04	0.03	0.04	0.06	0.03	0.07	0.06	0.02	0.03	0.02	0.10	0.06	0.03
CaO	1.47	0.92	1.23	0.71	0.63	0.72	0.58	1.11	0.94	1.15	0.85	0.63	0.67	1.06	0.43	1.94	0.33	0.53	0.72	0.62	0.62	0.94	0.66
Na_2O	2.51	2.48	2.51	2.60	3.06	2.67	2.66	2.74	2.52	2.66	3.09	3.00	2.52	2.60	0.30	2.18	1.97	1.59	2.70	2.53	1.84	2.17	0.40
K_2O	4.35	4.58	4.01	5.21	5.21	5.28	5.76	5.17	5.00	4.85	5.49	5.65	5.07	4.84	0.60	4.43	5.54	6.75	5.58	5.19	4.24	5.10	0.97
P_2O_5	0.18	0.16	0.19	0.28	0.13	0.26	0.26	0.17	0.19	0.16	0.13	0.17	0.22	0.20	0.04	0.20	0.13	0.42	0.13	0.12	0.16	0.19	0.10
P.F.	0.81	1.03	1.26	0.69	0.52	0.73	n.d.	n.d.	n.d.	n.d.	0.52	0.58	0.87	0.95	0.40	0.86	1.72	0.76	0.70	0.61	1.07	0.91	0.39
Total	100.23	99.63	99.72	99.42	100.38	99.78	97.28	96.90	96.99	97.20	99.53	100.66	100.20	99.25	1.32	99.92	99.45	99.90	100.25	99.34	99.77	99.67	0.41
A/(CNK)	1.26	1.33	1.40	1.26	1.20	1.27	1.18	1.14	1.26	1.20	1.13	1.16	1.32	1.25	0.09	1.23	1.63	1.35	1.21	1.24	1.63	1.36	0.19
Trace elements (ppm)																							
V	50	40	62	18	6	25	21	18	65	51	16	15	19	39	23	89	76	10	26	14	n.d.	46	34
Cr	106	74	114	83	60	35	17	135	64	83	15	28	85	64	34	90	63	8.8	20	14	n.d.	38	32
Rb	184	176	213	n.d.	200	230	280	138	222	240	194	204	n.d.	315	337	148	170	207	200	180	165	178	20
Sr	71	71	80	65	65	71	93	100	88	89	83	48	66	81	16	137	108	108	88	110	89	104	18
Y	19	10	15	24	11	23	28	19	12	11	13	11	24	27	19	26	14	18	15	12	25	23	14
Zr	45	44	37	92	42	101	110	78	123	86	86	82	92	106	61	n.d.	110	82	102	83	184	122	45
Nb	17	16	17	14	5.9	14	19	5.6	20	20	8.1	9.0	14	14	5	15	20	7.5	12	8.3	14	13	4
Ba	274	247	332	220	144	221	203	193	428	306	260	153	220	288	105	634	511	437	258	272	423	411	134
La	30	22	24	18	8.4	19	16	18	21	22	19	17	18	24	10	43	43	8.7	27	22	31	31	13
Ce	62	45	48	36	17	41	42	44	57	54	38	36	36	52	20	84	84	19	55	44	46	61	27
Pr	8.0	5.6	6.1	4.5	2.0	5.0	4.5	4.4	6.1	5.8	4.7	4.4	4.5	6.1	2.3	10.5	11.3	2.6	7.0	5.5	7.2	7.9	3.3
Nd	31	21	24	17	7.5	19	16	15	23	21	18	17	17	23	9	47	44	11	26	21	26	31	13
Sm	6.1	4.2	4.7	4.1	1.7	4.5	4.0	3.2	4.9	4.3	3.8	3.9	4.2	5.0	1.8	9.4	8.3	3.5	5.5	4.3	6.6	6.6	2.3
Eu	0.9	0.8	1.0	0.7	0.5	0.7	0.5	0.8	1.0	1.0	0.9	0.5	0.7	0.9	0.2	1.7	1.5	1.2	0.9	1.0	2.0	1.4	0.4
Gd	5.4	3.5	4.2	4.4	1.8	4.5	4.3	3.2	4.0	3.5	3.5	3.6	4.4	4.8	1.8	8.5	7.0	4.2	4.8	3.8	6.3	6.0	1.8
Tb	0.8	0.5	0.7	0.9	0.4	0.9	0.9	0.6	0.6	0.5	0.6	0.6	0.9	0.8	0.4	1.1	0.9	0.8	0.7	0.6	0.8	0.9	0.3
Dy	4.5	2.6	3.6	5.0	2.1	4.9	5.7	3.6	3.3	2.7	2.8	2.6	5.1	5.0	2.5	6.4	4.0	4.4	3.6	2.8	4.9	5.0	2.0
Ho	0.8	0.4	0.7	0.9	0.4	0.9	1.1	0.7	0.6	0.4	0.5	0.4	0.9	1.0	0.6	1.0	0.6	0.8	0.6	0.5	2.0	1.0	0.6
Er	2.0	1.1	1.7	2.5	1.3	2.5	2.9	2.2	1.2	1.0	1.3	1.0	2.5	2.7	1.9	2.8	1.4	1.8	1.5	1.2	2.9	2.4	1.4
Tm	0.27	0.16	0.25	0.38	0.22	0.39	0.45	0.34	0.16	0.15	0.20	0.15	0.38	0.40	0.26	0.24	0.19	0.26	0.22	0.17	0.49	0.33	0.22
Yb	1.6	1.0	1.5	2.4	1.5	2.5	2.7	2.0	1.1	1.0	1.3	0.9	2.4	2.5	1.6	2.0	1.0	1.5	1.4	1.1	3.0	2.1	1.3
Lu	0.22	0.15	0.23	0.38	0.24	0.39	0.43	0.31	0.15	0.14	0.21	0.15	0.38	0.37	0.23	0.15	0.17	0.23	0.21	0.18	0.40	0.28	0.18
Ta	4.0	5.0	4.3	2.2	1.7	2.3	3.7	2.2	5.9	5.2	2.0	1.7	2.2	3.0	1.4	4.5	2.4	2.0	2.2	1.8	n.d.	2.6	1.0
Pb	24	28	23	38	31	31	41	42	42	52	39	35	38	31	12	27	40	37	35	32	n.d.	34	5
Th	17	9.4	11	9.1	4.0	11	10	6.5	10	8.9	11	10	9.1	11	4	20	21	3.3	17	12	10	14	6
U	2.9	1.8	2.4	5.1	3.2	5.7	3.0	0.9	2.3	1.8	4.9	4.2	5.1	3.0	1.4	1.1	5.7	4.7	8.4	6.2	4.9	4.7	2.5

n.d. = not determined.

[a] Analyses carried out at Activation Laboratories Ltd. by ICP (for major elements) and ICP-MS (for trace elements); all other analyses carried out at the universities of Oviedo by XRF (for major elements) and Huelva by ICP-MS (for trace elements).

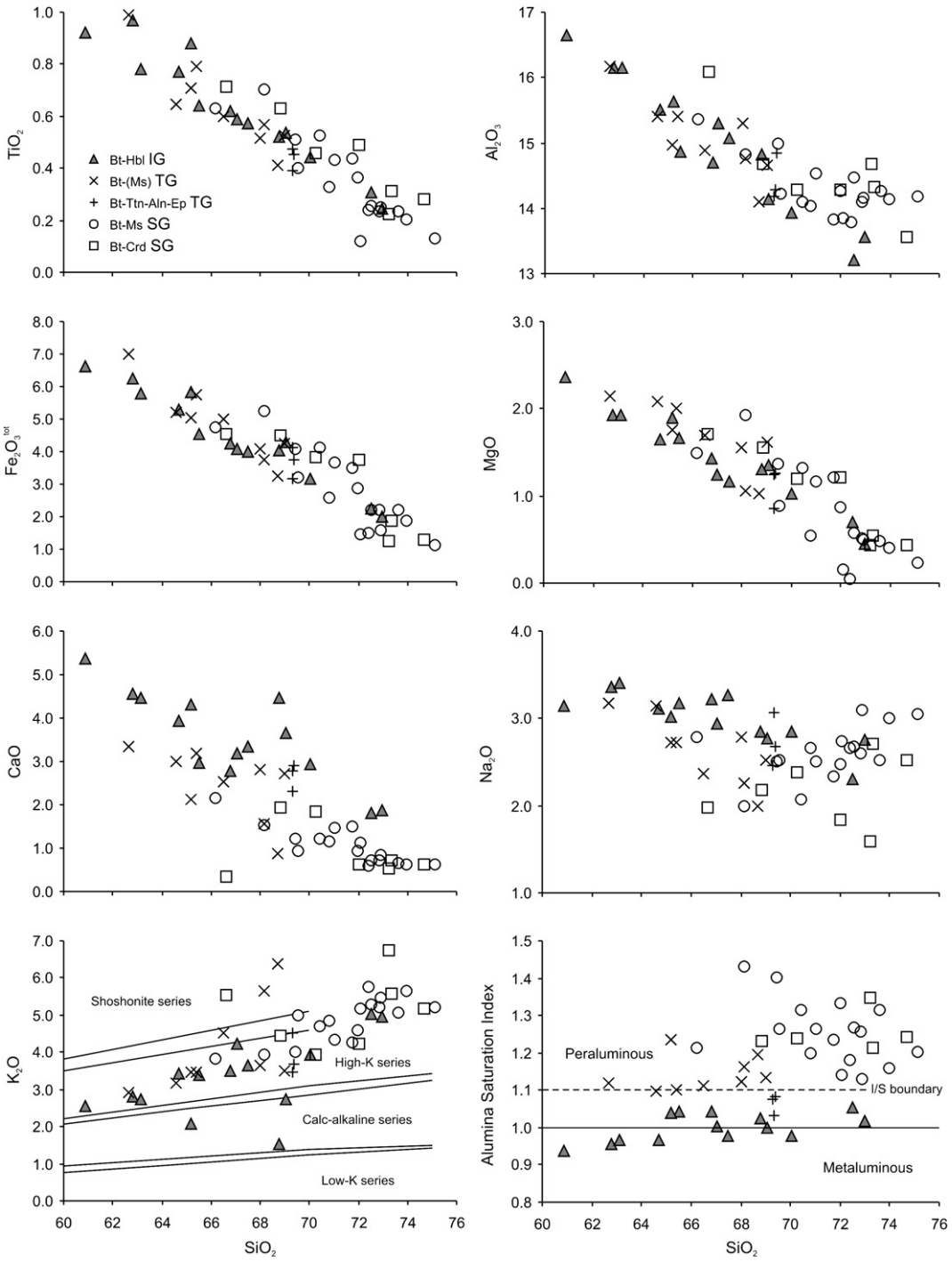

Fig. 3. Harker major oxides variation diagrams for the studied Sierra de Velasco granitoids. Fields in the K_2O vs. SiO_2 diagram are from Rickwood (1989). I/S-type granitoid boundary at ASI = 1.1 from Chappell and White (1974).

(trace elements), Spain. Major elements were determined by XRF with a Phillips PW2404 system using glass beads; the typical precision of this method is better than ±1.5%. Trace elements were analyzed by ICP-MS with an HP-4500 system. The precision and accuracy for most elements range between <5 and 10%, as determined by repeated analyses of international rock standards SARM-1 and SARM-4. Details on the procedures can be found at www.actlabs.com and in de la Rosa et al. (2001). The use of international standards at all labs ensures reproducibility and comparability of the resulting data. Previous analyses published in Bellos (2005; 11 samples of IG), Rossi et al. (2005; 3 samples of SG) and López et al. (2007; 2 samples of TG and 2 of SG) are also considered. Averages based on all samples are also shown in Table 1.

4.1. Major element geochemistry

The IG have the largest compositional range and are the least silicic granitoids (61–73% SiO_2). The TG have intermediate compositions (63–69% SiO_2), whereas the SG have the highest silica contents (66–75% SiO_2). On a K_2O vs. SiO_2 diagram, all three

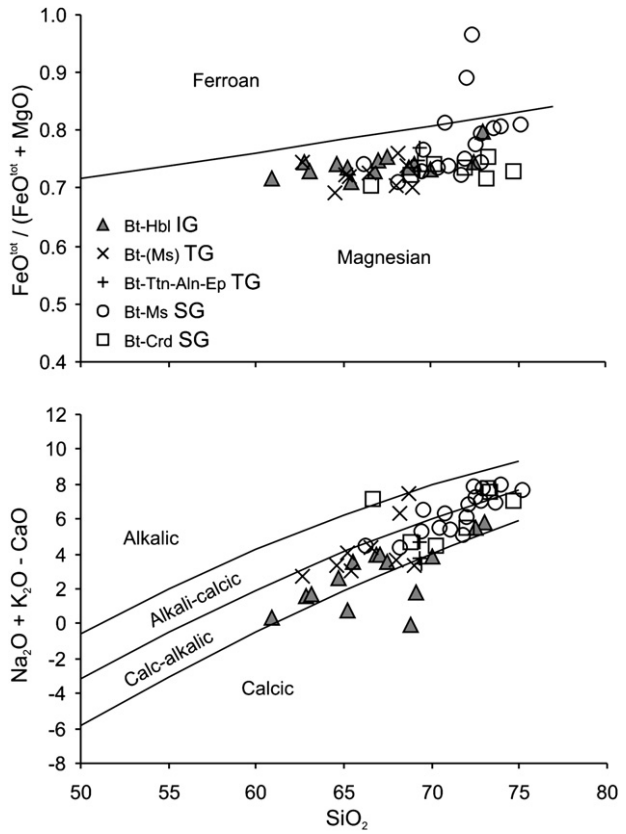

Fig. 4. Granite classification scheme of Frost et al. (2001) for the studied Sierra de Velasco granitoids.

granitoid types plot mostly in the high-K calc-alkaline field (Fig. 3). Following the classification scheme of Frost et al. (2001), they correspond to magnesian (Fig. 4a) and calc-alkalic granitoids (Fig. 4b). According to the alumina saturation index (ASI), the IG are metaluminous to weakly peraluminous (ASI = 0.94–1.05), the TG are moderately peraluminous (ASI = 1.03–1.24), and the SG are strongly peraluminous (ASI = 1.13–1.63) (Fig. 3).

The three granitoid types define different trends on the A–B diagram of Debon and Le Fort (1983) and plot in distinct fields following the classification of Villaseca et al. (1998) (Fig. 5). The IG plot in the metaluminous and low peraluminous fields and define a negative slope trend of increasing peraluminosity towards the more felsic samples. In contrast, the SG plot in the highly peraluminous field and have positive slope trends of decreasing peraluminosity towards the more felsic varieties; the biotite-cordierite variety roughly defines a steeper-sloped trend than the biotite–muscovite variety. The TG plot in the moderately peraluminous field and their trend is sub-horizontal, with fairly constant peraluminosity towards the more felsic samples.

On Harker variation diagrams, all three granitoid types show similar linear trends (Fig. 3). With increasing SiO_2 content, TiO_2, Al_2O_3, $Fe_2O_3^{tot}$, MgO, CaO and P_2O_5 decrease, whereas K_2O increases. Na_2O decreases in the IG and TG and shows an erratic behavior in the SG. The IG generally show better-defined trends, whereas the SG show the most scatter. Although the trends shown by the three granitoid types are similar, they are not continuous but are rather sub-parallel. Thus, for equal SiO_2 contents, the IG have higher concentrations of CaO and Na_2O and lower concentrations of TiO_2, Al_2O_3, $Fe_2O_3^{tot}$, MgO and P_2O_5 than the SG, whereas the TG usually have intermediate values.

The two varieties of the SG generally have similar major element concentrations. Mafic and felsic facies within the biotite–cordierite variety can be distinguished in the $Fe_2O_3^{tot}$ and MgO vs. SiO_2 diagrams (Fig. 3). The titanite–allanite–epidote TG variety is similar in composition to the main TG variety, although it is less peraluminous.

4.2. Trace element geochemistry

On variation diagrams, the trace elements tend to exhibit more scatter than the major elements and some trace elements show different behavior in the different granitoid types (Fig. 6).

In the IG, V, Sc, Sr, Eu and Zr show negative correlation with SiO_2, Rb a positive one, and Y, Nb and the HREE remain relatively constant. The Rb/Sr ratio is relatively low (average Rb/Sr = 0.8) and increases slightly with SiO_2. Compared to the other granitoid types, the IG are rich in Sr and Ba and poor in Rb.

The SG exhibit decreasing contents of V, Sr, Y, Ba, Zr and total REE, and increasing contents of Rb with increasing SiO_2. The Rb/Sr ratio also shows a positive correlation with SiO_2 (average Rb/Sr = 2.3). These granitoids are rich in Rb and poor in Sr and Ba. They are also relatively rich in Y and Th. The two SG varieties have similar trace element contents and they cannot be separated on these diagrams.

In the TG, trace elements generally show weak correlation with SiO_2, sometimes defining opposite trends with respect to the other granitoid types. V, Nb, Zr and Rb correlate negatively, whereas Ba correlates positively. Y and the REE do not exhibit obvious

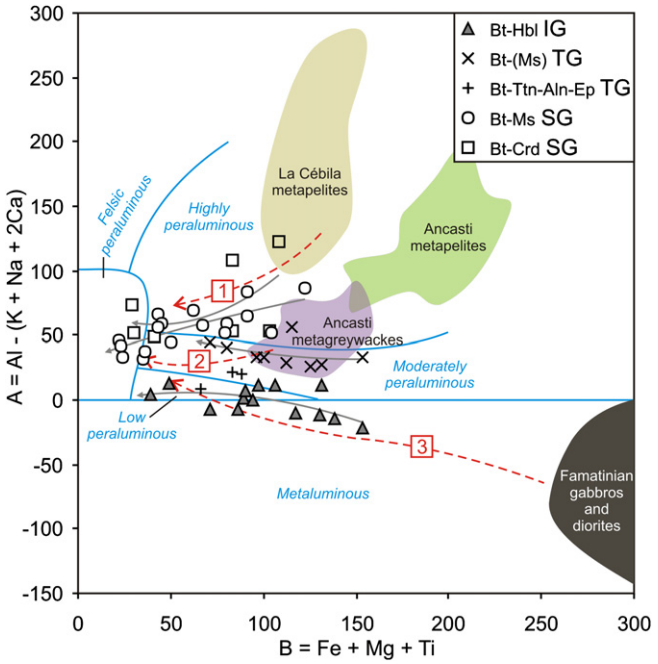

Fig. 5. A–B diagram of Debon and Le Fort (1983) for the studied Sierra de Velasco granitoids. Granitoid compositional fields in blue are from Villaseca et al. (1998). Solid gray arrows are the trends defined by each of the studied granitoid types (the three samples of the titanite–allanite–epidote TG variety were not considered for the calculation of the TG trend). Dashed red arrows are trends of experimental melts from different protoliths: 1 = pelite-derived melt (Vielzeuf and Holloway, 1988); 2 = greywacke-derived melt (Conrad et al., 1988); 3 = amphibolite-derived melt (Beard and Lofgren, 1991). Solid fields: La Cebila metapelites from Espizúa and Caminos (1979), Höckenreiner (1998) and our unpublished data; Ancasti metapelites from Willner et al. (1990); Ancasti metagreywackes from Willner et al. (1990) and our unpublished data; Famatinian gabbros and diorites from Pankhurst et al. (2000) (For interpretation of the references to color in this figure legend, the reader is referred to the web version of this article.).

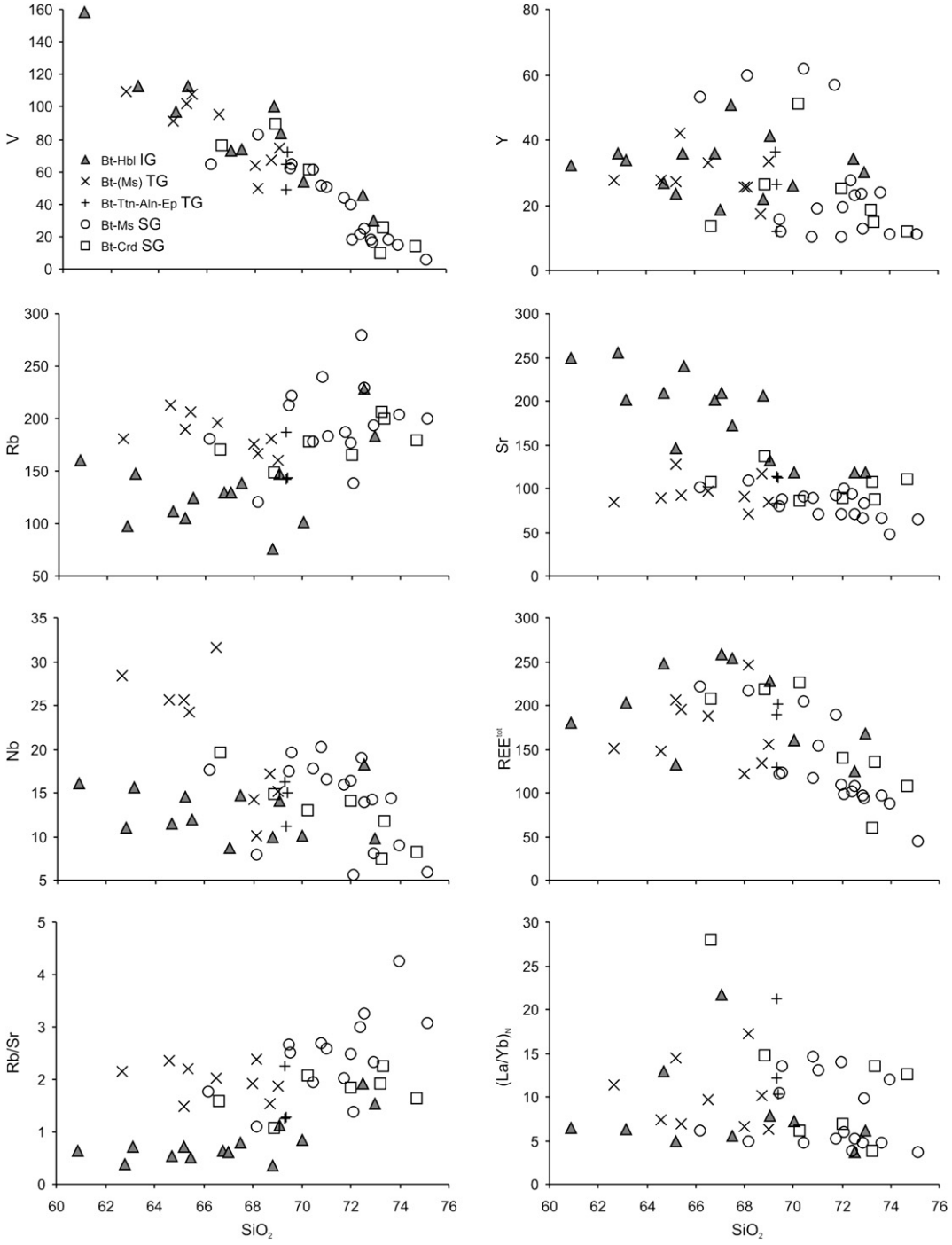

Fig. 6. Selected trace element variation diagrams for the studied Sierra de Velasco granitoids.

correlations with SiO_2. Rb and Ba trends are opposite to those of the other granitoid types. Sr values are quite constant, and the average Rb/Sr ratio is 1.9. Trace element concentrations are more similar to those of the SG than to those of the IG. The titanite–allanite–epidote TG variety generally has similar concentrations as the main TG variety.

REE chondrite-normalized plots are shown in Fig. 7. All granitoid types show relative LREE enrichment and HREE depletion, producing a concave-up pattern. They all have moderate negative Eu anomalies suggesting feldspar fractionation at the source. The negative Eu anomaly is generally less pronounced in the IG (average $Eu/Eu^* = 0.64$), and stronger in the TG (average $Eu/Eu^* = 0.54$) and the SG (average $Eu/Eu^* = 0.61$). In all granitoid types, REE fractionation tends to decrease with increasing SiO_2, although the correlation is generally not good. The IG usually have $(La/Yb)_N$ values of ~5–8, with the exception of three samples which have values >13, possibly related to higher allanite contents. The main TG variety has $(La/Yb)_N$ values of ~6–11, except two samples with values of 14 and 17, whereas the titanite-allanite-epidote variety has higher $(La/Yb)_N$ values of ~10–21, possibly related to higher monazite and allanite contents. The SG have very variable $(La/Yb)_N$ values ranging from 4 to 15. The biotite–muscovite SG generally

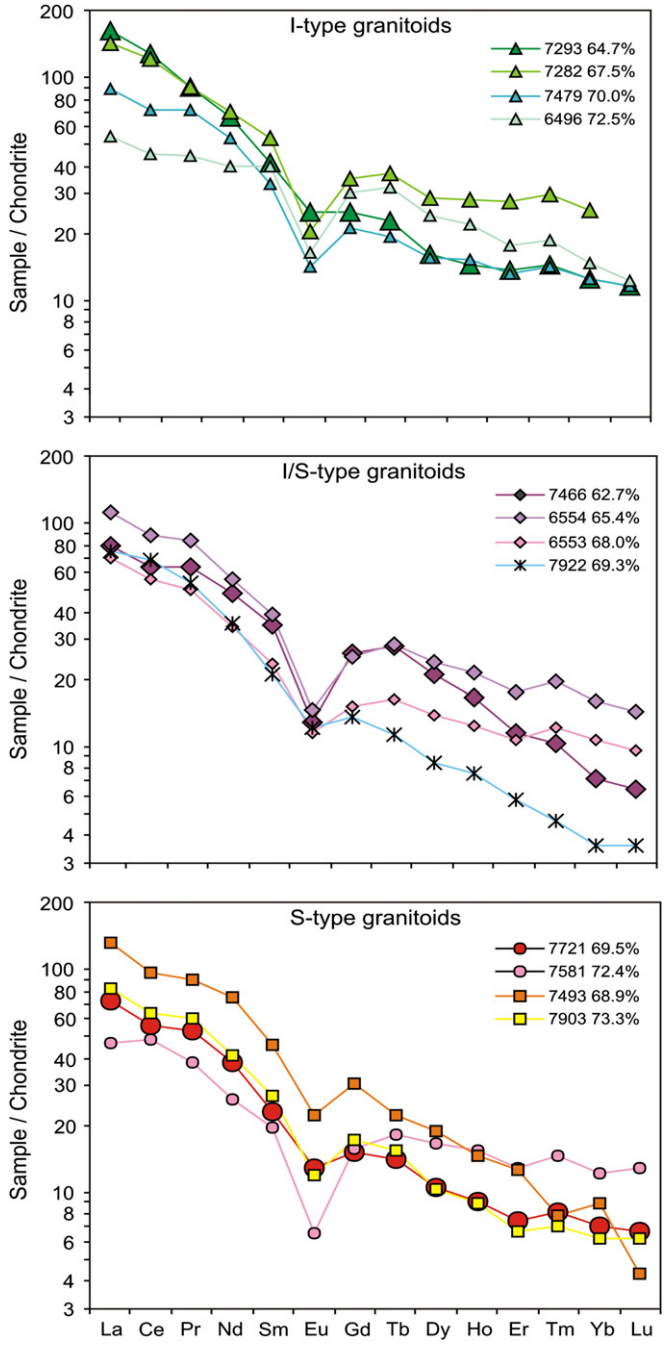

Fig. 7. Chondrite-normalized REE patterns for selected samples of the I-type, transitional I/S-type, and S-type granitoids of the Sierra de Velasco; SiO_2 contents of each sample are shown. Normalizing values from Nakamura (1974).

have higher HREE concentrations and lower $(La/Yb)_N$ values (average = 8), possibly related to higher garnet contents, whereas the biotite-cordierite SG generally have lower HREE contents and higher $(La/Yb)_N$ values (average = 10).

5. Nd isotopes

14 Whole-rock Nd isotope analyses of the studied granitoids are given in Table 2; locations are shown in Fig. 2. Four samples are of the IG, three of the TG and seven of the SG. Initial ratios are calculated using a crystallization age of 472 Ma, which is the average age of the granitoids based on all available U–Pb ages. Nine analyses were carried out at the Department of Earth and Environmental Sciences, Ludwig-Maximilians-Universität, Munich, Germany, and five at the Geochronology Laboratory of the Universidade de Brasilia, Brazil. Similar procedures were carried out at both labs, following the method described by Gioia and Pimentel (2000). Sm and Nd concentrations were determined by isotope dilution using a mixed Sm–Nd spike. Samples (50–100 mg) were dissolved with an HF–HNO_3 mixture and then with HCl 6 N. Sm and Nd were separated in Teflon columns by conventional cation exchange techniques. The isotopic ratios were measured on Re evaporation filaments using a Finnigan MAT 262 multi-collector mass spectrometer. εNd values were calculated using the CHUR constants of Goldstein et al. (1984) and Peucat et al. (1988). Two-stage model ages were calculated following Liew and Hofmann (1988).

The εNd values of all samples are negative, between −3.9 and −8.2, suggesting an isotopically evolved source or sources. The four IG samples have similar εNd values (−3.9 to −4.9) that are comparable to the values obtained for I-type granitoids of the sierras of southern La Rioja (Pankhurst et al., 1998; Fig. 8), although the IG values are slightly higher, suggesting a somewhat more primitive source and/or less contamination. The εNd values of the TG and SG are more variable and generally lower than those of the IG (Fig. 8). Two TG samples have values of −4.1 and −4.6 that are within the IG range, whereas the third sample has a lower value of −6.2. The SG samples span a wide range of values between −4.4 and −8.2 and all but one sample have values that are lower than the IG range. Most of the TG and SG εNd values are intermediate between those of the IG and those of metasedimentary basement rocks (Fig. 8), suggesting significant participation of crustal components in their genesis.

Two-stage Nd model ages of the three studied granitoid types are similar (Table 2): 1.46–1.54 Ga for the IG, 1.47–1.64 Ga for the TG, and 1.50–1.80 Ga for the SG. These ages are comparable to those determined for both I- and S-type Ordovician granitoids of neighboring ranges (~1.50–1.70 Ga; e.g. Pankhurst et al., 1998; Höckenreiner et al., 2003). The Nd model ages can be interpreted in two ways: (1) they indicate a Mesoproterozoic crustal source for the granitoids; (2) they reflect mixing between an older Palaeoproterozoic crustal source and a younger source.

6. Discussion

6.1. Classification of the granitoid types

Chappell and White (1974) first proposed the classification of granites into I- and S-types, based on studies of the Lachlan Fold Belt granites of eastern Australia. Although this classification has its pitfalls (e.g. Clarke, 1992), it is valid in that it recognizes that highly contrasting parental materials can be involved in the genesis of granites and that granites image these sources, although not necessarily in a simple manner (e.g. Clemens, 2003). I-types are considered to be derived by melting of metaigneous crust, whereas S-types are considered to derive from melting of metasedimentary crust. The main criteria for distinguishing I- and S-types can be summarized as follows (see Chappell and White, 1974, 1992, 2001): I-types usually contain hornblende and titanite and have mafic microgranular enclaves. They are metaluminous to weakly peraluminous (ASI < 1.1) and have higher concentrations in Ca, Na and Sr. Their εNd values range from +3.5 to −8.9. S-types contain Al-rich minerals (muscovite, cordierite, garnet, sillimanite, andalusite) and have metasedimentary enclaves. They are always peraluminous (ASI > 1.1) and have higher contents in K and Rb. Their εNd values range from −5.8 to −9.2.

Table 2
Whole-rock Sm–Nd isotope data of the studied Sierra de Velasco granitoids.

Sample	Sm (ppm)	Nd (ppm)	$^{143}Nd/^{144}Nd$	2σ error	$^{147}Sm/^{144}Nd$	εNd (472 Ma)	Nd two-stage model age (Ga)
I-type granitoids							
6999[a]	7.35	33.2	0.512223	0.000009	0.1338	−4.3	1.49
7145[a]	16.6	115	0.512047	0.000029	0.0873	−4.9	1.54
7293[a]	8.39	41.4	0.512191	0.000005	0.1225	−4.3	1.49
7479[a]	5.41	28.8	0.512182	0.000007	0.1134	−3.9	1.46
Transitional I/S-type granitoids							
7466[a]	5.83	25.9	0.512216	0.000014	0.1358	−4.6	1.51
7682[a]	5.25	34.4	0.512106	0.000009	0.0922	−4.1	1.47
7920[b]	11.4	51.3	0.512128	0.000014	0.1345	−6.2	1.64
S-type Bt-Ms granitoids							
7359[a]	2.82	16.7	0.512083	0.000008	0.1020	−5.1	1.56
7688[a]	4.72	26.3	0.512138	0.000007	0.1085	−4.4	1.50
7833[b]	4.16	21.5	0.512024	0.000014	0.1170	−7.2	1.72
7907[b]	4.00	16.5	0.512078	0.000009	0.1463	−7.9	1.77
S-type Bt-Crd granitoids							
7493[a]	8.10	41.0	0.512113	0.000006	0.1194	−5.6	1.59
7663[b]	3.03	9.26	0.512219	0.000011	0.1978	−8.2	1.80
7903[b]	5.46	25.7	0.512024	0.000018	0.1285	−7.9	1.77

εNd values calculated asuming $^{143}Nd/^{144}Nd\ (CHUR)_{today} = 0.512638$ (Goldstein et al., 1984) and $^{147}Sm/^{144}Nd\ (CHUR)_{today} = 0.1967$ (Peucat et al., 1988). Calculation of 2-stage model ages after Liew and Hofmann (1988) with $^{143}Nd/^{144}Nd\ (DM) = 0.513151$, $^{147}Sm/^{144}Nd\ (DM) = 0.219$ and $^{147}Sm/^{144}Nd\ (CC) = 0.12$.

[a] Analyses carried out at the Department of Earth and Environmental Sciences, Ludwig-Maximilians-Universität, Munich, Germany.

[b] Analyses carried out at the Geochronology Laboratory of the Universidade de Brasilia, Brazil.

Following these criteria, the IG are clearly I-type granites and the SG are S-type granites. Classification of the TG is more difficult: (a) they lack hornblende but sometimes contain titanite and they usually, but not always, contain scarce muscovite; (b) they contain both metasedimentary and mafic enclaves; (c) they have ASI values slightly above or below 1.10 (the average is 1.12); (d) their chemistry is intermediate between the IG and SG, generally more similar to the later; and (e) their εNd values are comparable to both the SG and IG. The TG clearly have intermediate or transitional characteristics between the other two granite types and thus can hardly be classified as either I- or S-type. They can be regarded more accurately as transitional I/S-type granitoids, or as hybrid granitoids following the classification scheme and nomenclature proposed by Castro et al. (1991). This scheme recognizes the importance of magma mixing or hybridization in the origin of granitoids in orogenic environments by introducing a new category of H-type (hybrid) granitoids. Considering mantle-derived magmas and anatectic melts as mixing end-members, the classification scheme consists of mafic, totally mantle-derived granitoids (M-type), felsic, totally metasedimentary-derived granitoids (S-type), and three intermediate H-type granitoid classes: H_m-type, in which the contribution of the mafic magma predominates; H_s-type, in which the felsic end-member predominates; and H_{ss}-type (hybrid *sensu stricto*), in which the participation of each end-member is more or less equal. Following this scheme, the TG would classify as H_{ss}-type, the IG as H_m-type and the SG as H_s-type.

6.2. Origin of the three granitoid types

The more primitive IG samples (i.e. those with lower SiO_2 content) are invariably metaluminous and rich in Fe_2O_3, MgO, CaO and Sr. Villaseca et al. (1998) indicate that these compositions cannot be generated by partial melting of any peraluminous crustal protolith such as metapelites, metagreywackes or acid metaigneous rocks, and that the only possible protholiths are metabasic rocks such as basaltic amphibolites. Comparison of the IG with compositions of melts produced by experimental dehydration-melting of various lithologies supports this idea (Figs. 5 and 9). The compositional trend shown by the IG on the A–B diagram is similar to the trend produced by the experimental melting of an amphibolite under water-undersaturated, lower crustal conditions performed by Beard and Lofgren (1991, Fig. 5). These authors showed that 30% amphibolite melting produces a tonalitic melt with A–B values of −36 and 180, which are very similar to the values of the more primitive IG samples. Furthermore, in most major element diagrams designed by Patiño Douce (1999), the IG samples plot in the field corresponding to melts derived from amphibolites (Fig. 9). However, the IG, and Cordilleran calc-alkaline granitoids in general, tend to have higher K/Na ratios compared to basaltic amphibolite derived melts (Fig. 9), suggesting either (1) assimilation of basaltic melts with metasediments, or (2) re-melting of older calc-alkaline rocks that were themselves formed by basalt magma – metasediment interaction (Wolf and Wyllie, 1991; Patiño Douce, 1999; Castro et al., 1999). The εNd values of the IG samples are considerably lower than the εNd values of gabbros from the Sierra de Valle Fértil, considered by Pankhurst et al. (2000) and Otamendi et al. (2009a) as potential sources for I-type granitoids, and mostly higher than the εNd values of high-grade crustal metasediments of the Sierras Pampeanas (Fig. 8), thus agreeing with a process of interaction of mafic melts with crustal medasediments in their genesis.

Strongly peraluminous granites such as the SG can be generated by partial melting of metasediments, either pelites or greywackes, and/or acid metaigneous rocks (i.e. peraluminous orthogneisses, e.g. Miller, 1985; Holtz and Johannes, 1991; Villaseca et al., 1998). In the A–B diagram (Fig. 5), the biotite-muscovite SG compositional trend plots between the trends of experimental melts derived from

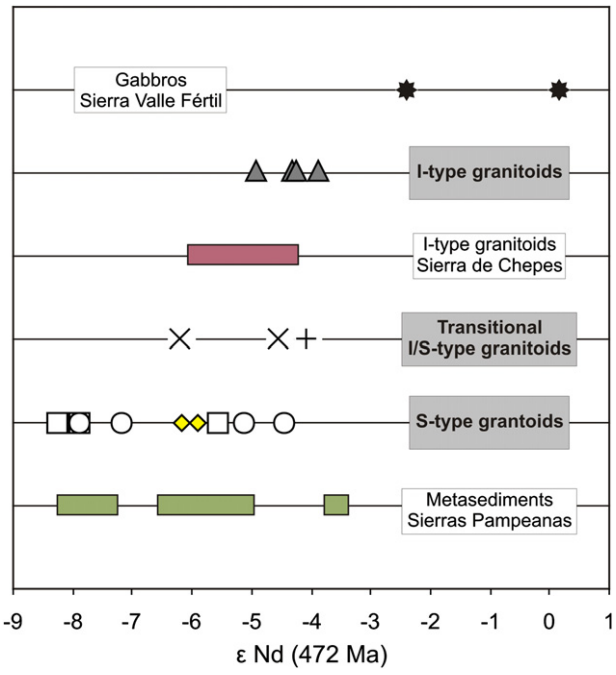

Fig. 8. εNd values (472 Ma) of the studied Sierra de Velasco granitoid types (symbols as in Fig. 3). Diamonds are S-type granitoids from the Sierras of Copacabana and Fiambalá (from Höckenreiner et al., 2003). Field of Sierra de Chepes I-type granitoids from Pankhurst et al. (1998); field of Sierras Pampeanas metasediments from Pankhurst et al. (1998), Rapela et al. (1998) and Becchio (2000); Sierra de Valle Fértil gabbros from Pankhurst et al. (2000) and Otamendi et al. (2009a).

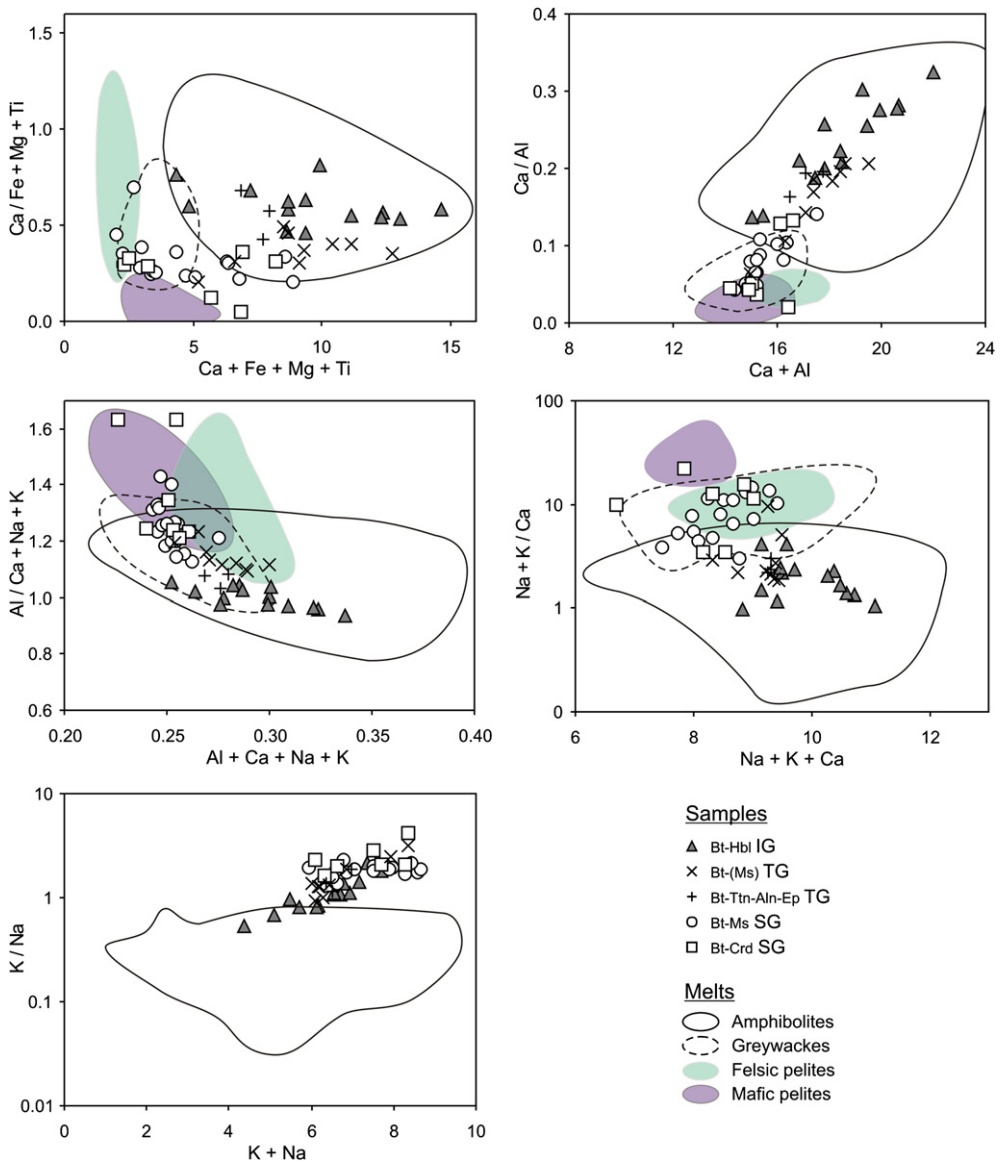

Fig. 9. Major element diagrams modified from Patiño Douce (1999), with compositions of the studied Sierra de Velasco granitoids. Fields are compositions of experimental dehydration-melting of various lithologies (for source of data see Patiño Douce, 1999).

metapelites and metagreywackes, suggesting derivation from a mixture of both protoliths. This is consistent with field observations indicating that the metasediments that form the metamorphic basement of NW Argentina (Puncoviscana Formation s.l.) consist of intercalating pelite-greywacke sequences (Willner et al., 1990; Do Campo and Guevara, 2005). The biotite-cordierite SG trend suggests a more metapelitic source and/or assimilation with a metapelitic host-rock, such as the La Cébila Formation, during emplacement. Abundant metamorphic xenoliths, roof pendants and xenocrystic cordierite within some biotite-cordierite SG bodies support the possibility of considerable contamination by the La Cébila Formation. Comparison with melts in the diagrams of Patiño Douce (1999) (Fig. 9) indicates that the SG have concentrations of alumina and alkalis compatible with a metasedimentary origin, but their concentrations of calcium and especially the ferromagnesian components are too high. These values can be explained either by interaction with mafic magmas (e.g. Elburg, 1996; Castro et al., 1999) or incorporation of restitic phases (White and Chappell, 1977). The presence of mafic enclaves, and the lack of metasedimentary restites, support the participation of mafic material. The involvement of a mafic component in the genesis of the SG is consistent with their Nd isotopic ratios, since the SG samples have εNd values that are mostly intermediate between the IG and basement metasediments (Fig. 8). The high variability of the SG εNd values can be linked to the isotopic heterogeneity shown by the metasedimentary end-members (Fig. 8).

The TG have intermediate compositions between the IG and the SG. In the A–B diagram, they define a sub-horizontal trend of constant peraluminosity with increasing differentiation, between the trends of the IG and SG; their compositions are similar to those of metagreywackes (Fig. 5). Comparing the trend of the TG with melts produced by metapelites and metagreywackes it is clear that the TG are not pure melts of either of these protoliths: their peraluminosities are too low compared with pelite-derived melts and they are too mafic compared with both types of melts. A mafic component seems to be necessary in their genesis. This is further supported when the TG are compared with experimental melts in the diagrams of Patiño Douce (1999) (Fig. 9). The TG samples

generally plot in the field of amphibolitic-derived melts, indicating that they are too rich in calcium and ferromagnesian components to be of a purely metasedimentary origin. The presence of mafic enclaves supports the participation of a mafic component. The εNd values of the two samples from the main TG variety are within the SG range, whereas one of these samples and the titanite-allanite-epìdote TG sample have values within the IG range (Fig. 8). The TG εNd values are thus not conclusive and can concur with the participation of either or both the SG and IG in their formation. The intermediate composition of the TG suggests a hybrid or mixed origin, as was already suggested by Pankhurst et al. (2000) for biotite granites on the southwestern flank of the sierra. Their formation can be explained in two ways: (1) "first generation" mixing of mafic and metasedimentary melts, and (2) "second generation" mixing of IG and SG melts.

6.3. Geotectonic implications: across-arc variation of Famatinian magmatism

Available U–Pb ages constrain the timing of Famatinian magmatism in the Sierra de Velasco to ~480–460 Ma and indicate that the production of I-, S- and transitional I/S-type granitoids was broadly coeval, in agreement with regional geochronological studies (e.g. Pankhurst et al., 2000). Thus, the across-arc variation of Famatinian magmatism does not seem to be time dependent. Instead, the variation from I- to S-type granitoids towards the continental interior is likely related to varying genetic processes within a single and continuous subduction-related setting.

All three studied granitoid types have negative εNd values and similar old Nd model ages of ~1.6 Ga suggesting similar, mostly isotopically evolved, sources. The compositions of the different granitoid types can be explained by the varying participation of two main sources: (1) mafic lower crust/lithospheric mantle; and (2) metasedimentary crust. The across-arc variation from I- to I/S- to S-type granitoids can be envisaged as the result of a progressive increase in the participation of the metasedimentary component towards the interior of the continent, probably at progressively higher crustal levels and related with increasing crustal thickness. Following this interpretation, a continuous across-arc magmatic variation would be expected, as has been proposed for other subduction-related arcs (e.g. Gray, 1984; Liew and Hofmann, 1988; Collins, 1996, 1998). However, transitional I/S-type granitoids seem to be much scarcer than I- and S-type granitoids, both in the Famatinian arc and in arcs in general. This suggests that, although there is a progressive compositional variation in general terms, two end-member situations are more likely: (1) mafic lower crust melting and production of metaluminous magmas, with minor metasedimentary contamination, towards the continental margin; and (2) melting of metasedimentary crust with minor assimilation of mafic melts generating strongly peraluminous magmas towards the continental interior. The intermediate case of mixing of the two end-members, and consequent formation of transitional I/S-type melts, is possibly less common because it may only occur at spatially limited intermediate zones where batches of already produced I- and S-type magmas pond and mix.

The different granitoid types were emplaced at different crustal levels, although all at relatively shallow depths. The biotite-muscovite SG and the TG emplaced at ~14–18 km depths (Rossi and Toselli, 2004; Rossi et al., 2005; de los Hoyos et al., in press), whereas the IG emplaced at shallower levels (Bellos et al., 2010, estimate a maximum depth of ~12 km), along with the biotite–cordierite SG (~10 km; de los Hoyos et al., in press). The shallower emplacement level of the IG compared to the biotite–muscovite SG and the TG may be related to more favorable tectonic conditions towards the continental margin and/or the lower viscosity and higher temperatures of the I-type magmas.

After emplacement, all of the granitoid types suffered regional-scale deformation resulting in the observed foliations. NNW–SSE trending shear zones later developed, along which the granitoids were probably displaced and relocated to their present positions. The more deeply emplaced TG and biotite–muscovite SG may have been displaced upwards relative to the IG and placed in contact by reverse westward movements along the shear zones (e.g. López et al., 2006).

7. Summary and conclusions

The Sierra de Velasco is a key area for the across-arc reconstruction of the subduction-related Famatinian magmatism since it comprises continuous outcrops ranging from I- to S-type granitoids. The sierra contains three main types of Early Ordovician granitoids that reflect the across-arc variation of Famatinian magmatism. The three granitoid types are mineralogically and geochemically distinct but as a whole make up a continuous high-K, magnesian and calc-alkalic magmatic series with similar trace element contents.

The IG are biotite–hornblende–titanite metaluminous to weakly peraluminous granodiorites and tonalites typical of the coastal I-type granitoid belt and can be correlated with the granitoids of the sierras of Famatina, southern La Rioja and Valle Fértil; they were possibly formed by melting of mafic lower crust/lithospheric mantle, with minor assimilation of crustal metasediments. The SG are biotite–muscovite and subordinate biotite–cordierite strongly peraluminous syeno- and monzogranites representative of the S-type belt; they likely formed by large-scale anatexis of metasedimentary crust and hybridization with the more mafic lower crustal melts. The TG are biotite, biotite–muscovite and subordinate biotite–titanite–allanite–epidote moderately peraluminous I/S-type monzogranites, granodiorites and tonalities that are here recognized and characterized for the first time in the Famatinian arc; they show intermediate characteristics between the I- and S-type granitoids and were possibly generated by less common mechanisms of mixing between I-type and S-type magmas and/or their parent melts of mafic lower crustal and metasedimentary melts.

The IG have rather constant Nd isotopic ratios reflecting their mostly mafic lower crustal source. In contrast, the SG and TG show higher isotopic variability that can be related with the very large isotopic variability of the middle and upper metasedimentary crust of the Sierras Pampeanas, which participated significantly in their genesis. This variability is consistent with the higher major and trace element scatter of the TG and SG compositions.

The transition from IG to TG to SG implies a compositional continuum related to an increasing participation of crustal metasediments towards the continental interior, as has been proposed in other arcs (e.g. DePaolo, 1981; Brown et al., 1984; Gray, 1984; Liew and Hofmann, 1988; Collins, 1996). However, two main aspects differentiate the Famatinian across-arc variation from that of other arcs: (1) the different types of magmatism are synchronous, as opposed to being progressively younger inland (e.g. Miller and Bradfish, 1980) or younger outboard (e.g. Collins and Richards, 2008), and (2) there seems to be no, or minor, involvement of juvenile material/asthenosphere, a major component in other arcs (e.g. Miller and Bradfish, 1980; Collins, 1996; Castro et al., 1999). Instead, the sources of the studied granitoids seem to consist of mafic lower crust/lithospheric mantle and crustal metasediments in variable proportions (see also Pankhurst et al., 2000; Viramonte et al., 2007).

This study shows that a two-way I-type and S-type classification may not be fully adequate when across-arc magmatism is studied

with some detail. Progressive variations related to different degrees of mixing between mafic and metasedimentary end-members produce a wide range of fairly continuous compositions instead of a clear-cut separation. In this case, a more suitable classification would be that of the H-type (hybrid) granitoids proposed by Castro et al. (1991).

Acknowledgements

We are grateful to Jesus de la Rosa for carrying out several of the whole-rock chemical analyses in Spain. Frank Söllner and Alex Rocholl are thanked for their help with the Nd isotope analyses in Munich. We also thank Frank Söllner and Antonio Castro for commenting on earlier versions of the manuscript. P. Grosse acknowledges the Consejo Nacional de Investigaciones Científicas y Técnicas (CONICET) and the Deutscher Akademischer Austauschdienst (DAAD) for scholarships awarded during his PhD studies. The Consejo de Investigaciones of the Universidad Nacional de Tucumán (CIUNT) is thanked for financial support through projects 26/G321 and 26/G439. Thorough reviews by Damian Nance and Robert Pankhurst helped improve the quality of the manuscript.

References

Aceñolaza, F.G., Toselli, A.J., 1973. Consideraciones estratigráficas y tectónicas sobre el Paleozoico inferior del Noroeste Argentino. In: Proceedings II Congreso Latinoamericano de Geología, Caracas, Venezuela, pp. 755–763.

Aceñolaza, F.G., Toselli, A.J., 1981. Geología del Noroeste Argentino. In: Facultad de Ciencias Naturales, UNT, Tucumán, Special Publications, vol. 1287, 212 pp.

Aceñolaza, F.G., Miller, H., Toselli, A.J. (Eds.), 1996. Geología del Sistema de Famatina. Münchner Geologische Hefte, Reihe A19, Munich. 410 pp.

Aceñolaza, F.G., Miller, H., Toselli, A.J., 2002. Proterozoic–Early Paleozoic evolution in western South America: a discussion. Tectonophysics 354, 121–137.

Adams, C.J., Miller, H., Toselli, A.J., 1990. Nuevas edades de metamorfismo por el método K-Ar de la Formación Puncoviscana y equivalentes, NW de Argentina. In: Aceñolaza, F.G., Miller, H., Toselli, A.J. (Eds.), El Ciclo Pampeano en el Noroeste Argentino. Serie Correlación Geológica, 4, pp. 209–219.

Astini, R.A., Benedetto, J.L., Vaccari, N.E., 1995. The Early Paleozoic evolution of the Argentine Precordillera as a Laurentian rifted, drifted, and collided terrane: a geodynamic model. Geological Society of America Bulletin 107, 253–273.

Bachmann, G., Grauert, B., Miller, H., 1986. Isotopic dating of polymetamorphic metasediments from Northwest Argentina. Zentralblatt für Geologie und Paläontologie, Teil I (Heft 9/10), 1257–1268.

Báez, M.A., Basei, M.A., Rossi, J.N., Toselli, A.J., 2008. Geochronology of Paleozoic magmatic events in northern Sierra de Velasco, Argentina. In: Proceedings VI South American Symposium on Isotope Geology, Bariloche, Argentina, pp. 66.

Báez, M.A., Bellos, L.I., Grosse, P., Sardi, F.G., 2005. Caracterización petrológica de la sierra de Velasco. In: Dahlquist, J.A., Rapela, C.W., Baldo, E. (Eds.), Geología de la provincia de La Rioja – Precámbrico-Paleozoico Inferior. Asociación Geológica Argentina, Special Publications Serie D, vol. 8, pp. 123–130.

Báez, M.A., Rossi, J.N., Sardi, F.G., 2002. Consideraciones preliminares sobre los granitoides del norte de la Sierra de Velasco, La Rioja, Argentina. In: Proceedings XV Congreso Geológico Argentino, El Calafate, Argentina, vol. II, pp. 69–74.

Bahlburg, H., 1998. The geochemistry and provenance of Ordovician turbidites in the Argentine Puna. In: Pankhurst, R.J., Rapela, C.W. (Eds.), The Proto-Andean Margin of Gondwana. Geological Society, London, Special Publications, vol. 142, pp. 127–142.

Bahlburg, H., Hervé, F., 1997. Geodynamic evolution and tectonostratigraphic terranes of northwestern Argentina and northern Chile. Geological Society of America Bulletin 109, 869–884.

Beard, J.S., Lofgren, G.E., 1991. Dehydration melting and water-saturated melting of basaltic and andesitic greenstones and amphibolites at 1, 3, and 6.9 kbar. Journal of Petrology 32, 365–401.

Becchio, R., 2000. Petrología y geoquímica del basamento del borde oriental de la Puna Austral. Ph.D. Thesis, Universidad Nacional de Salta, 128 p..

Bellos, L.I., 2005. Geología del sector sur de la sierra de Velasco, La Rioja. In: Aceñolaza, F.G., Aceñolaza, G., Hünicken, M., Rossi, J.N., Toselli, A.J. (Eds.), Simposio Bodenbender. Serie Correlación Geológica, vol. 19, pp. 261–278.

Bellos, L.I., 2008. Petrología de los granitoides del sur de la Sierra de Velasco y su significación regional. Ph.D. Thesis, Universidad Nacional de Córdoba, 334 p..

Bellos, L.I., Grosse, P., Ruiz, A., Rossi, J.N., Toselli, A.J., 2002. Petrografía y geoquímica de granitoides del flanco sud-occidental de la Sierra de Velasco, La Rioja, Argentina. In: Proceedings XV Congreso Geológico Argentino, vol. II, El Calafate, Argentina, pp. 81–86.

Bellos, L.I., Toselli, A.J., Rossi, J.N., Grosse, P., de la Rosa, J.D., Castro, A., 2010. Caracterización petrográfica y geoquímica y condiciones de deformación del plutón San Cristóbal, Sierra de Velasco (La Rioja, Argentina). Estudios Geológicos 66, 157–169.

Bock, B., Bahlburg, H., Worner, G., Zimmermann, U., 2000. Tracing crustal evolution in the southern Central Andes from Late Precambrian to Permian with geochemical and Nd and Pb isotope data. The Journal of Geology 108, 515–535.

Brown, G.C., Thorpe, R.S., Webb, P.C., 1984. The geochemical characteristics of granitoids in contrasting arcs and comments on magma sources. Journal of the Geological Society of London 141, 413–426.

Büttner, S.H., Glodny, J., Lucassen, F., Wemmer, K., Erdmann, S., Handler, R., Franz, G., 2005. Ordovician metamorphism and plutonism in the Sierra de Quilmes metamorphic complex: implications for the tectonic setting of the northern Sierras Pampeanas (NW Argentina). Lithos 83, 143–181.

Castro, A., Moreno-Ventas, I., de la Rosa, J.D., 1991. H-type (hybrid) granitoids: a proposed revision of the granite-type classification and nomenclature. Earth-Science Reviews 31, 237–253.

Castro, A., Patiño Douce, A.E., Corretgé, L.G., de la Rosa, J.D., El-Biad, M., El-Hmidi, H., 1999. Origin of peraluminous granites and granodiorites, Iberian Massif, Spain: an experimental test of granite petrogenesis. Contributions to Mineralogy and Petrology 135, 255–276.

Chappell, B.W., White, A.J.R., 1974. Two contrasting granite types. Pacific Geology 8, 173–174.

Chappell, B.W., White, A.J.R., 1992. I- and S-type granites in the Lachlan Fold Belt. Transactions of the Royal Society of Edinburgh: Earth Sciences 83, 1–26.

Chappell, B.W., White, A.J.R., 2001. Two contrasting granite types: 25 years later. Australian Journal of Earth Sciences 48, 489–499.

Chernicoff, C.J., Zappettini, E.O., Santos, J.O.S., Allchurch, S., McNaughton, N.J., 2010. The southern segment of the Famatinian magmatic arc, La Pampa Province, Argentina. Gondwana Research 17, 662–675.

Clarke, D.B., 1992. Granitoid Rocks. Chapman & Hall, London. 283 p..

Clemens, J.D., 2003. S-type granitic magmas–petrogenetic issues, models and evidence. Earth-Science Reviews 61, 1–18.

Cobbing, E.J., Mallick, D.I.J., Pitfield, P.E.J., Teoh, L.H., 1986. The granites of the Southeast Asian tin belt. Journal of the Geological Society of London 143, 537–550.

Coira, B., Pérez, B., Flores, P., Kay, S.M., Woll, B., Hanning, M., 1999. Magmatic sources and tectonic setting of Gondwana margin Ordovician magmas, northern Puna of Argentina and Chile. In: Ramos, V., Keppie, J. (Eds.), Laurentia-Gondwana connections before Pangea. Geological Society of America, Special Papers, vol. 336, pp. 145–170.

Collins, W.J., 1996. Lachlan Fold Belt granitoids: products of three-component mixing. Transactions of the Royal Society of Edinburgh: Earth Sciences 87, 171–179.

Collins, W.J., 1998. Evaluation of petrogenetic models for Lachlan Fold Belt granitoids: implications for crustal architecture and tectonic models. Australian Journal of Earth Sciences 45, 483–500.

Collins, W.J., Richards, S.W., 2008. Geodynamic significance of S-type granites in circum-Pacific orogens. Geology 36, 559–562.

Conrad, W.K., Nicholls, I.A., Wall, V.J., 1988. Water-saturated and undersaturated melting of metaluminous and peraluminous crustal composition at 10 kb: evidence for the origin of silicic magmas in the Taupo Volcanic Zone, New Zealand, and other occurrences. Journal of Petrology 29, 765–803.

Dahlquist, J.A., Alasino, P.H., Eby, G.N., Galindo, C., Casquet, C., 2010. Fault controlled Carboniferous A-type magmatism in the proto-Andean foreland (Sierras Pampeanas, Argentina): geochemical constraints and petrogenesis. Lithos 115, 65–81.

Dahlquist, J.A., Pankhurst, R.J., Rapela, C.W., Casquet, C., Fanning, C.M., Alasino, P., Báez, M.A., 2006. The San Blas Pluton: an example of Carboniferous plutonism in the Sierras Pampeanas, Argentina. Journal of South American Earth Sciences 20, 341–350.

Dahlquist, J.A., Pankhurst, R.J., Rapela, C.W., Galindo, C., Alasino, P., Fanning, C.M., Saavedra, J., Baldo, E.G., 2008. New SHRIMP U–Pb data from the Famatina Complex: constraining Early–Mid Ordovician Famatinian magmatism in the Sierras Pampeanas, Argentina. Geologica Acta 6, 319–333.

de la Rosa, J.D., Chacón, H., Sánchez de la Campa, A., Carrasco, R., Nieto, J.M., 2001. Metodología y análisis de elementos trazas-REE mediante ICP-MS del standard SARM 1 granito y SARM 4 norita. In: Proceedings III Congreso Ibérico de Geoquímica, Zaragoza, Spain, pp. 435–438.

de los Hoyos, C.R., Willner, A.P., Larrovere, M.A., Rossi, J.N., Toselli, A.J., Basei, M.A.S. Tectonothermal evolution and exhumation history of the Paleozoic Proto-Andean Gondwana margin crust: the Famatinian Belt in NW Argentina. Gondwana Research, in press. doi:10.1016/j.gr.2010.12.004.

Debon, F., Le Fort, P., 1983. A chemical–mineralogical classification of common plutonic rocks and associations. Transactions of the Royal Society of Edinburgh: Earth Sciences 73, 135–149.

DePaolo, D.J., 1981. Trace element and isotopic effects of combined wallrock assimilation and fractional crystallization. Earth and Planetary Science Letters 53, 189–202.

Do Campo, M., Guevara, S., 2005. Provenance analysis and tectonic setting of late Neoproterozoic metasedimentary successions in NW Argentina. Journal of South American Earth Sciences 19, 143–153.

Elburg, M.A., 1996. Genetic significance of multiple enclave types in a peraluminous ignimbrite suite, Lachlan Fold Belt, Australia. Journal of Petrology 37, 1385–1408.

Espizúa, S., Caminos, R., 1979. Las rocas metamórficas de la Formación La Cébila, Sierra de Ambato, Provincias de Catamarca y La Rioja. Boletín de la Academia Nacional de Ciencias, Córdoba 53, 125–142.
Fershater, G.B., Bea, F., Borodina, N.S., Montero, P., 1998. Lateral zonation, evolution, and geodynamic interpretation of magmatism of the Urals: new petrological and geochemical data. Petrology 6, 409–433.
Finney, S.C., Gleason, J.D., Gehrels, G.E., Peralta, S., Aceñolaza, G., 2003. Early Gondwanan connection for the Argentine Precordillera terrane. Earth and Planetary Science Letters 205, 349–359.
Finney, S.C., Gleason, J.D., Gehrels, G.E., Peralta, S., Aceñolaza, G., 2004. Corrigendum to "Early Gondwanan connection for the Argentine Precordillera terrane". Earth and Planetary Science Letters 219, 413.
Frost, B.R., Barnes, C.G., Collins, W.J., Arculus, R.J., Ellis, D.J., Frost, C.D., 2001. A geochemical classification for granitic rocks. Journal of Petrology 42, 2033–2048.
Gioia, S.M.C.L., Pimentel, M.M., 2000. The Sm–Nd isotopic method in the geochronology laboratory of the University of Brasília. Anais da Academia Brasília de Ciencias 72, 219–245.
Goldstein, S.L., O'Nions, R.K., Hamilton, P.J., 1984. A Sm–Nd study of atmospheric dusts and particulates from major river systems. Earth and Planetary Science Letters 70, 221–236.
González Bonorino, F., 1950. Algunos problemas geológicos de las Sierras Pampeanas. Revista de la Asociación Geológica Argentina 5, 81–110.
González Bonorino, F., 1951. Una nueva formación Precámbrica en el noroeste Argentino. Comunicaciones Científicas, Museo de La Plata 5.
Gray, C.M., 1984. An isotopic mixing model for the origin of granitic rocks in southeastern Australia. Earth and Planetary Science Letters 70, 47–60.
Grissom, G.C., De Bari, S.M., Lawrence, W.S., 1998. Geology of the Sierra de Fiambalá, northwestern Argentina: implications for Early Paleozoic Andean tectonics. In: Pankhurst, R.J., Rapela, C.W. (Eds.), The Proto-Andean margin of Gondwana. Geological Society of London, Special Publications, vol. 142, pp. 297–323.
Grosse, P., Sardi, F.G., 2005. Geología de los granitos Huaco y Sanagasta, sector centro-oriental de la Sierra de Velasco, La Rioja. In: Aceñolaza, F.G., Aceñolaza, G., Hünicken, M., Rossi, J.N., Toselli, A.J. (Eds.), Simposio Bodenbender. Serie Correlación Geológica, vol. 19, pp. 221–238.
Grosse, P., Söllner, F., Báez, M.A., Toselli, A.J., Rossi, J.N., de la Rosa, J.D., 2009. Lower Carboniferous post-orogenic granites in central-eastern Sierra de Velasco, Sierras Pampeanas, Argentina: U–Pb monazite geochronology, geochemistry and Sr-Nd isotopes. International Journal of Earth Sciences 98, 1001–1025.
Höckenreiner, M., 1998. Die Formation La Cébila und ihr geologisches Umfeld (Sierra de Ambato, NW Argentinien). Undergraduate Thesis, Ludwig-Maximilians-Universität, Munich, 96 p..
Höckenreiner, M., Söllner, F., Miller, H., 2003. Dating the TIPA shear zone: an Early Devonian terrane boundary between Famatinian and Pampean systems (NW-Argentina). Journal of South American Earth Sciences 16, 45–66.
Holtz, F., Johannes, W., 1991. Genesis of peraluminous granites I. Experimental investigation of melt compositions at 3 and 5 kb and various H_2O activities. Journal of Petrology 32, 935–958.
Isacks, B., 1988. Uplift of the central Andean plateau and bending of the Bolivian Orocline. Journal of Geophysical Research B93, 3211–3231.
Ježek, P., 1990. Análisis sedimentológico de la Formación Puncoviscana entre Tucumán y Salta. In: Aceñolaza, F.G., Miller, H., Toselli, A.J. (Eds.), El Ciclo Pampeano en el Noroeste Argentino. Serie Correlación Geológica, vol. 4, pp. 9–36.
Jordan, T.E., Allmendinger, R.W., 1986. The Sierras Pampeanas of Argentina: a modern analogue of Rocky Mountain foreland deformation. American Journal of Science 286, 737–764.
Larrovere, M.A., de los Hoyos, C.R., Toselli, A.J., Rossi, J.N., Basei, M.A.S., Belmar, M.E., 2011. High T/P evolution and metamorphic ages of the migmatitic basement of northern Sierras Pampeanas, Argentina: characterization of a mid-crustal segment of the Famatinian belt. Journal of South American Earth Sciences 31, 279–297.
Liew, T.C., Hofmann, A.W., 1988. Precambrian crustal components, plutonic associations, plate environment of the Hercynian Fold Belt of central Europe: indications from a Nd and Sr isotopic study. Contributions to Mineralogy and Petrology 98, 129–138.
Llambías, E.J., Sato, A.M., Ortiz Suárez, A., Prozzi, C., 1998. The granitoids of the Sierra de San Luis. In: Pankhurst, R.J., Rapela, C.W. (Eds.), The Proto-Andean margin of Gondwana. Geological Society of London, Special Publications, vol. 142, pp. 325–341.
López, J.P., Toselli, A.J., 1993. La faja milonítica Tipa: faldeo oriental del Sistema de Famatina, Argentina. In: Proceedings XII Congreso Geológico Argentino, Mendoza, Argentina, vol. III 39–42.
López, J.P., Bellos, L.I., Grosse, P., 2006. Estructura y petrografía de zonas de cizalla en la sierra de Velasco, La Rioja. In: Asociación Geológica Argentina, Special Publications Serie D, vol. 10 201–206.
López, J.P., Grosse, P., Toselli, A.J., 2007. Faja de deformación La Horqueta, Sierra de Velasco, Sierras Pampeanas, NO de Argentina: petrografía, geoquímica, estructuras y significado tectónico. Estudios Geológicos 63, 5–18.
López, J.P., Sales, A., Basei, M.A., 2000. Sistemática Nueva edad K/Ar en la historia deformativa de la Faja Milonítica Tipa, en el Noroeste Argentino. Zentralblatt für Geologie und Paläontologie, Teil I (Heft 7/8), 895–902.
Lork, A., Miller, H., Kramm, U., Grauert, B., 1990. Sistemática U–Pb de circones detríticos de la Formación Puncoviscana y su significado para la edad máxima de sedimentación en la sierra de Cachi (provincia de Salta, Argentina). In: Aceñolaza, F.G., Miller, H., Toselli, A.J. (Eds.), El Ciclo Pampeano en el Noroeste Argentino. Serie Correlación Geológica, vol. 4, pp. 209–219.
Lucassen, F., Becchio, R., 2003. Timing of high-grade metamorphism: Early Paleozoic U-Pb formation ages of titanite indicate long-standing high-T conditions at the western margin of Gondwana (Argentina, 26–29° S). Journal of Metamorphic Geology 21, 649–662.
Miller, C.F., 1985. Are strongly peraluminous magmas derived from pelitic sedimentary sources? The Journal of Geology 93, 673–689.
Miller, C.F., Bradfish, L.J., 1980. An inner Cordilleran belt of muscovite-bearing plutons. Geology 8, 412–416.
Miller, H., Söllner, F., 2005. The Famatina complex (NW-Argentina): back-docking of an island arc or terrane accretion? Early Palaeozoic geodynamics at the western Gondwana margin. In: Vaughan, A.P.M., Leat, P.T., Pankhurst, R.J. (Eds.), Terrane Processes at the Margins of Gondwana. Geological Society of London, Special Publications, vol. 246, pp. 241–256.
Nakamura, N., 1974. Determination of REE, Ba, Mg, Na and K in carbonaceous and ordinary chondrites. Geochimica et Cosmochimica Acta 38, 757–773.
Otamendi, J.E., Ducea, M.N., Tibaldi, A.M., Bergantz, G.W., de la Rosa, J.D., Vujovich, G.I., 2009a. Generation of tonalitic and dioritic magmas by coupled partial melting of gabbroic and metasedimentary rocks within the deep crust of the Famatinian magmatic arc, Argentina. Journal of Petrology 50, 841–873.
Otamendi, J.E., Vujovich, G.I., de la Rosa, J.D., Tibaldi, A.M., Castro, A., Martino, R.D., Pinotti, L.P., 2009b. Geology and petrology of a deep crustal zone from the Famatinian paleo-arc, Sierras de Valle Fértil and La Huerta, San Juan, Argentina. Journal of South American Earth Sciences 27, 258–279.
Pankhurst, R.J., Rapela, C.W., 1998. The proto-Andean margin of Gondwana: an introduction. In: Pankhurst, R.J., Rapela, C.W. (Eds.), The Proto-Andean Margin of Gondwana. Geological Society of London, Special Publications, vol. 142, pp. 1–10.
Pankhurst, R.J., Rapela, C.W., Fanning, C.M., 2000. Age and origin of coeval TTG, I- and S-type granites in the Famatinian belt of NW Argentina. Transactions of the Royal Society of Edinburgh: Earth Sciences 91, 151–168.
Pankhurst, R.J., Rapela, C.W., Saavedra, J., Baldo, E.G., Dahlquist, J.A., Pascua, I., Fanning, C.M., 1998. The Famatinian arc in the central Sierras Pampeanas: an early to mid-Ordovician continental arc on the Gondwana margin. In: Pankhurst, R.J., Rapela, C.W. (Eds.), The Proto-Andean Margin of Gondwana. Geological Society of London, Special Publications, vol. 142, pp. 343–367.
Patiño Douce, A.E., 1999. What do experiments tell us about the relative contributions of crust and mantle to the origin of granitic magmas? In: Castro, A., Fernández, C., Vigneresse, J.L. (Eds.), Understanding Granites: Integrating New and Classical Techniques Geological Society of London, Special Publications, vol. 168, pp. 55–75.
Peucat, J.J., Vidal, P., Bernard-Griffiths, J., Condie, K.C., 1988. Sr, Nd and Pb isotopic systematics in the Archean low- to high-grade transition zone of southern India: syn-accretion vs. post-accretion granulites. The Journal of Geology 97, 537–550.
Pieters, P., Skirrow, R.G., Lyons, P., 1997. Informe geológico y metalogénico de las Sierras de Las Minas, Chepes y Los Llanos (provincia de La Rioja), 1:250.000. In: Anales XXVI, Instituto de Geología y Recursos Minerales, SEGEMAR, Buenos Aires, Argentina.
Poma, S., Quenardelle, S., Litvak, V., Maisonnave, E.B., Koukharsky, M., 2004. The Sierra de Macón, plutonic expression of the Ordovician magmatic arc, Salta Province, Argentina. Journal of South American Earth Sciences 16, 587–597.
Prozzi, C., 1990. Consideraciones acerca del basamento de San Luis, Argentina. In: Proceedings XI Congreso Geológico Argentino, San Juan, Argentina, vol. I, pp. 452–455.
Ramos, V.A., 1988. Late Proterozoic–Early Paleozoic of South America: a collisional history. Episodes 11, 168–174.
Ramos, V.A., 2004. Cuyania, an exotic block to Gondwana: review of a historical success and the present problems. Gondwana Research 7, 1009–1026.
Rapela, C.W., Pankhurst, R.J., Baldo, E.G., Casquet, C., Galindo, C., Fanning, C.M., Saavedra, J., 2001. Ordovician metamorphism in the Sierras Pampeanas: new U–Pb SHRIMP ages in central-east Valle Fertil and the Velasco Batholith. In: Proceedings III South American Symposiun on Isotope Geology, Pucón, Chile Article 616, 1–4 (CD).
Rapela, C.W., Pankhurst, R.J., Casquet, C., Baldo, E.G., Saavedra, J., Galindo, C., Fanning, C.M., 1998. The Pampean Orogeny of the southern proto-Andes: evidence for Cambrian continental collision in the Sierras de Córdoba. In: Pankhurst, R.J., Rapela, C.W. (Eds.), The Proto-Andean Margin of Gondwana. Geological Society of London, Special Publications, vol. 142, pp. 181–217.
Rapela, C.W., Pankhurst, R.J., Casquet, C., Fanning, C.M., Baldo, E.G., González-Casado, J.M., Galindo, C., Dahlquist, J.A., 2007. The Río de La Plata craton and the assembly of SW Gondwana. Earth-Science Reviews 83, 49–82.
Rapela, C.W., Pankhurst, R.J., Kirschbaum, A., Baldo, E.G., 1991. Facies intrusivas de edad carbónica en el Batolito de Achala: Evidencia de una anatexis regional en las Sierras Pampeanas?. In: Proceedings VI Congreso Geológico Chileno, Viña del Mar, Chile, vol. I, pp. 40–43.
Rapela, C.W., Toselli, A.J., Heaman, L., Saavedra, J., 1990. Granite plutonism of the Sierras Pampeanas: an inner cordilleran Paleozoic arc in the southern Andes. In: Kay, S.M., Rapela, C.W. (Eds.), Plutonism from Antarctica to Alaska. Geological Society of America, Special Papers, vol. 241, pp. 77–90.
Rickwood, P.C., 1989. Boundary lines within petrologic diagrams which use oxides of mayor and minor elements. Lithos 22, 247–263.
Rossi, J.N., Toselli, A.J., 2004. Termobarometría de las corneanas granatíferas del flanco sudoccidental de la sierra de Velasco, La Rioja, Argentina. In: Proceedings VII Congreso de Mineralogía y Metalogenia, Río Cuarto, Argentina, pp. 403–408.

Rossi, J.N., Toselli, A.J., Báez, M.A., 2005. Evolución termobárica del ortogneis peraluminoso del noroeste de la sierra de Velasco, La Rioja. Revista de la Asociación Geológica Argentina 60, 278–289.

Rossi, J.N., Toselli, A.J., López, J.P., 2000. Deformación y metamorfismo en el noroeste de la sierra de Velasco, La Rioja, Argentina. Zentralblatt für Geologie und Paläontologie, Teil 1 (Heft 7/8), 839–850.

Rossi, J.N., Toselli, A.J., Saavedra, J., Sial, A.N., Pellitero, E., Ferreira, V.P., 2002. Common crustal source for contrasting peraluminous facies in the Early Paleozoic Capillitas Batholith, NW Argentina. Gondwana Research 5, 325–337.

Saavedra, J., Toselli, A.J., Rossi, J.N., Pellitero, E., Durand, F., 1998. The Early Paleozoic magmatic record of the Famatina system: a review. In: Pankhurst, R.J., Rapela, C.W. (Eds.), The Proto-Andean Margin of Gondwana. Geological Society of London, Special Publications, vol. 142, pp. 283–295.

Schalamuk, I.B., Toselli, A.J., Saavedra, J., Echeveste, H., Fernández, R., 1989. Geología y mineralización del sector Este de la Sierra de Mazán, La Rioja, Argentina. Revista de la Asociación Argentina de Mineralogía, Petrología y Sedimentología 20, 1–12.

Shaw, S.E., Flood, R.H., 1981. The New England Batholith, eastern Australia: geochemical variations in time and space. Journal of Geophysical Research B86, 10530–10544.

Sibson, C., 1977. Fault rocks and fault mechanisms. Journal of the Geological Society of London 133, 191–221.

Siegesmund, S., Steenken, A., López de Luchi, M.G., Wemmer, K., Hoffmann, A., Mosch, S., 2004. The Las Chacras-Potrerillos batholith (Pampean Ranges, Argentina): structural evidences, emplacement and timing of the intrusión. International Journal of Earth Sciences 93, 23–43.

Sims, J.P., Ireland, T.R., Camacho, A., Lyons, P., Pieters, P.E., Skirrow, R.G., Stuart-Smith, P.G., 1998. U–Pb, Th–Pb and Ar–Ar geochronology from the southern Sierras Pampeanas, Argentina: implications for the Palaeozoic tectonic evolution of the western Gondwana margin. In: Pankhurst, R.J., Rapela, C.W. (Eds.), The Proto-Andean Margin of Gondwana. Geological Society of London, Special Publications, vol. 142, pp. 259–281.

Steenken, A., Siegesmund, S., Wemmer, K., López de Luchi, M.G., 2008. Time constraints on the Famatinian and Achalian structural evolution of the basement of the Sierra de San Luis (Eastern Sierras Pampeanas, Argentina). Journal of South American Earth Sciences 25, 336–358.

Thomas, W.A., Astini, R.A., 2003. Ordovician accretion of the Argentine Precordillera terrane to Gondwana: a review. Journal of South American Earth Sciences 16, 67–79.

Toselli, A.J., 1990. Metamorfismo del Ciclo Pampeano. In: Aceñolaza, F.G., Miller, H., Toselli, A.J. (Eds.), El Ciclo Pampeano en el Noroeste Argentino. Serie Correlación Geológica, vol. 4, pp. 181–198.

Toselli, A.J., Durand, F., Rossi, J.N., Saavedra, J., 1996. Esquema de evolución geotectónica y magmática eopaleozoica del Sistema de Famatina y sectores de Sierras Pampeanas. In: Proceedings XIII Congreso Geológico Argentino, Buenos Aires, Argentina, vol. 5 443–462.

Toselli, A.J., Miller, H., Aceñolaza, F.G., Rossi, J.N., Söllner, F., 2007. The Sierra de Velasco (northwestern Argentina) – an example for polyphase magmatism at the margin of Gondwana. Neues Jahrbuch für Geologie und Paläontologie 246, 325–345.

Toselli, A.J., Rossi, J.N., Miller, H., Báez, M.A., Grosse, P., López, J.P., Bellos, L.I., 2005. Las rocas graníticas y metamórficas de la Sierra de Velasco. In: Aceñolaza, F.G., Aceñolaza, G., Hünicken, M., Rossi, J.N., Toselli, A.J. (Eds.), Simposio Bodenbender. Serie Correlación Geológica, vol. 19, pp. 211–220.

Toselli, G., Saavedra, J., Córdoba, G., Medina, M., 1991. Petrología y geoquímica de lo granitos de la zona Carrizal-Mazán, La Rioja-Catamarca. Revista de la Asociación Geológica Argentina 46, 36–50.

Turner, J.C.M., 1960. Estratigrafía de la Sierra de Santa Victoria y adyacencias. Boletín de la Academia Nacional de Ciencias, Córdoba 41, 163–196.

Varela, R., Basei, M.A., Pereyra, C.P., 2008. Datación U–Pb del granito Paimán, Sierra de Paimán, Chilecito, La Rioja. Revista de la Asociación Geológica Argentina 63, 97–101.

Vaughan, A.P.M., Pankhurst, R.J., 2008. Tectonic overview of the West Gondwana margin. Gondwana Research 13, 150–162.

Verdecchia, S.O., Baldo, E.G., Benedetto, J.L., Borghi, P.A., 2007. The first shelly faunas from metamorphic rocks of the Sierras Pampeanas (La Cébila Formation, Sierra de Ambato, Argentina): age and paleogeographic implications. Ameghiniana 44, 493–498.

Vielzeuf, D., Holloway, J.R., 1988. Experimental determination of the fluid-absent melting relations in the pelitic system. Consequences for crustal differentiation. Contributions to Mineralogy and Petrology 98, 257–276.

Villaseca, C., Barbero, L., Herreros, V., 1998. A re-examination of the typology of peraluminous granite types in intracontinental orogenic belts. Transactions of the Royal Society of Edinburgh: Earth Sciences 89, 113–119.

Viramonte, J.M., Becchio, R.A., Viramonte, J.G., Pimentel, M.M., Martino, R.D., 2007. Ordovician igneous and metamorphic units in southeastern Puna: new U–Pb and Sm–Nd data and implications for the evolution of northwestern Argentina. Journal of South American Earth Sciences 24, 167–183.

Von Gosen, W., Prozzi, C., 1998. Structural evolution of the Sierra de San Luis (Eastern Sierras Pampeanas, Argentina): implications for the proto-Andean margin of Gondwana. In: Pankhurst, R.J., Rapela, C.W. (Eds.), The Proto-Andean Margin of Gondwana. Geological Society of London, Special Publications, vol. 142, pp. 235–258.

White, A.J.R., Chappell, B.W., 1977. Ultrametamorphism and granitoid genesis. Tectonophysics 43, 7–22.

Whitney, D.L., Evans, B.W., 2010. Abbreviations for names of rock-forming minerals. American Mineralogist 95, 185–187.

Willner, A.P., Miller, H., Jezek, P., 1990. Composición geoquímica del basamento sedimentario-metamórfico de los Andes del NW Argentino (Precámbrico superior-Cámbrico inferior). In: Aceñolaza, F.G., Miller, H., Toselli, A.J. (Eds.), El Ciclo Pampeano en el Noroeste Argentino. Serie Correlación Geológica, vol. 4, pp. 161–179.

Wolf, M.B., Wyllie, P.J., 1991. Dehydration-melting of solid amphibolite at 10 kbar: Textural development, liquid interconnectivity and applications to the segregation of magmas. Mineralogy and Petrology 44, 151–179.